E.ON Energy Research Center

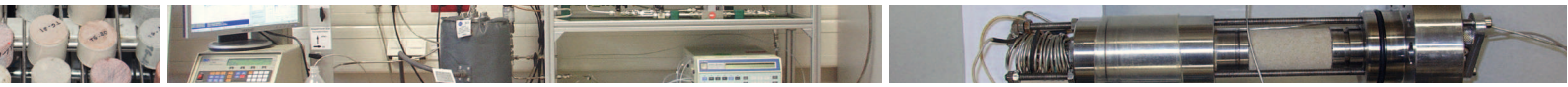

E.ON Energy Research Center Series

Physical Properties of Rocks – Installation of a high Pressure, high Temperature Test Facility

Rainer Schütt, Norbert Klitzsch, Christoph Clauser

Volume 6, Issue 2

RWTH AACHEN UNIVERSITY

E.ON Energy Research Center

E.ON Energy Research Center Series

Physical Properties of Rocks – Installation of a high Pressure, high Temperature Test Facility

Rainer Schütt, Norbert Klitzsch, Christoph Clauser

Volume 6, Issue 2

RWTH AACHEN UNIVERSITY

Physical Properties of Rocks – Installation of a high Pressure, high Temperature Test Facility

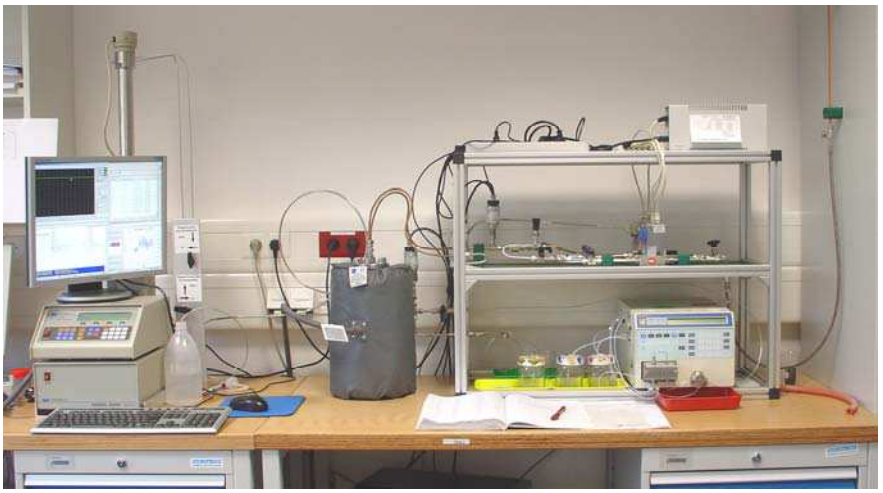

Rainer Schütt, Norbert Klitzsch, Christoph Clauser

Institute for Applied Geophysics and Geothermal Energy
E.ON Energy Research Center
RWTH Aachen

E.ON ERC gGmbH Projekt-Nr. 18

September 2013

RWTH AACHEN UNIVERSITY

E.ON Energy Research Center

APPLIED GEOPHYSICS AND GEOTHERMAL ENERGY

Physical Properties of Rocks –
Installation of a high Pressure, high Temperature Test Facility

Contents

Physical Properties of Rocks – Installation of a high Pressure, high Temperature Test Facility

Summary

Rocks are inhomogeneous materials. Physical properties vary on large scale as well as between samples. Mineral composition, pore fluid, and depth of origin are some of the influencing variables. Information on the variance of the rock properties is important for both geophysical exploration and for modelling.

A set-up was assembled for the determination of important physical properties at various influencing conditions. This report describes the measuring system and results obtained.

Permeability of low permeability rocks is measured at confining pressures from 3 MPa to 25 MPa. Measurements are made with Argon gas and converted to fluid-independent permeability according to Klinkenberg (e.g. Schön 1996), measuring range $5x10^{-18}$ m^2 to $2x10^{-12}$ m^2. As no measurements were performed at atmospheric confining pressure, permeability is plotted logarithmically versus pressure for conversion to ambient pressure. Additionally a measuring cycle is illustrated for temperatures between room temperature and 150 °C.

In long term experiments, permeability measured with water as flowing fluid yielded decreasing values. This was found for tap, distilled and saline water and different rock types. This is caused by biogenic films in the pore space of some clean quartz sandstones. In other rocks this could be caused also by swelling of clay minerals. The reduction of permeability lies in the range of 50 % to 90 %. Special is the decreasing of permeability with decreasing flow.

For measuring ultrasonic wave propagation velocities the sample size of 30 mm diameter and a length of 30 mm to 50 mm and the grain limit the frequencies of compressional and shear waves to some 100 kHz to 2 MHz. Velocity increases with increasing confining pressures. Applying of a pore pressure results in reducing the overall stress, and the ultrasonic velocities equal those measured at the corresponding reduced confining pressure.

1. Motivation

Physical properties of rocks are important input parameters in different branches of science and technology. For exploration of hydrocarbon, geothermal, and mineral reservoirs, as well as for subsurface storage of nuclear waste or CO_2 knowledge of lithological parameters is essential.

Pressure (p) and temperature (T) inside the earth increase with depth. In many regions at a depth of 3000 m temperature is around 90 °C to 100 °C, the lithostatic overburden pressure reaches about 100 MPa (= 1 kbar; rock density 2500 kg/m^3 to 3000 kg/m^3), and pore pressure

30 MPa or more (water density 1000 kg/m^3). Physical properties of porous rocks vary strongly with pressure. Porosity and permeability decrease with pressure while velocity of shear- and compressional waves increases. Samples brought to the surface from deep boreholes are affected by the drilling itself and, in particular, by the pressure release. Both results in an opening of pre-existing cracks and in the generation of new cracks. This affects at most all physical properties. Laboratory measurements at elevated confining pressure help to reduce or prevent these effects.

Rocks are inhomogeneous media. Generally speaking, their internal structure varies with location and depth. The description of the internal structure, the grains and pores, can be only approximately. Relations between two or more physical rock parameter are based upon laboratory measurements and until now, more or less are descriptive in character or based approximations of responsible physical effects.

At confining pressure of 10 MPa to 20 MPa cracks resulting from pressure release after hauling to surface are predominantly closed. Further pressure increase changes the physical properties like permeability and ultrasonic velocities in most cases only slightly. So an apparatus for measuring relevant physical properties at confining pressures up to 40 MPa (400 bar) was constructed.

2. Permeability measured with Argon gas

Permeability describes how easily a fluid flows through a porous material. Rock permeability can be determined by measuring the flow of a liquid or gaseous fluid through a sample. Darcy (1856) developed the fluid flow equation for this problem.

$$Q = \frac{k * A}{\eta * l} \Delta p \qquad \text{(Eq. 1)}$$

Q = volume flow rate, k = permeability, η = dynamic viscosity, Δp = pressure difference between inflow and outflow, l = length of sample, A = cross section.

Flow through and pressure decrease between in- and outflow of a sample (differential pressure) are the main measured variables. Additional parameters are temperature of the fluid for determining the fluid viscosity and the size of the sample (length, cross section area) (e.g. Schön 1996).

Noble gases are ideal fluids for measuring the permeability k because no interactions occur between fluid and minerals. But gas molecules move through the pore space different from fluid molecules. In capillaries, the velocity of liquids increases from zero at the wall to a maximum in the centre. In contrast gas molecules at the wall are additionally in motion in flow direction. This increases the flow rate and has to be taken into account when using gas. Klinkenberg found a way to resolve this phenomenon of the so called “molecular slip” by measuring gas flow at different gas pressures (e.g. Schön 1996). With increasing gas pressure p_i the calculated pressure dependent permeability $k(p_i)$ approaches the liquid value.

$k(p_i) = k(p \rightarrow \infty)(1 + b/p_i)$ (Eq. 2)

b = slip factor

A linear regression of permeability $k(p_i)$ versus reciprocal pressure $1/p_i$ yields k for $1/p = 0$, i.e. is $p \rightarrow \infty$.

2.1 Gas-permeability : Experimental setup

The apparatus constructed for gas flow measurements is displayed in Figure 1. A gas cylinder with pressure-reducing regulators provides the noble gas Argon at pressures between about 0.1 MPa and 1 MPa. Five flowmeter with overlapping measuring ranges (Bronkhorst EL-FLOW 2 mL/min to 100 L/min) measure the gas flow (volume and temperature), and a pressure transducer the gas pressure at the inlet and when working at an elevated pressure level another one at the outlet.

The rock sample inside the autoclave is separated from the pressure medium by a rubber sleeve. In our case, water is used for the high pressure confining circuit. Because of its much lower compressibility it is less dangerous than gas at pressures of some 10 MPa. Safety features, such as a back-pressure valve and blow-out disk, protect the measuring devices if a sample casing breaks.

For preventing bypass-flow along the sample surface, heat shrinking tubes are used. Thin latex finger used as a first layer, in order to prevent glue of the shrinking tube from contaminating the surface and penetrating into the pore space. In connection with the elevated confining pressure, surface irregularities have therefore a minor influence. Confining pressures of 3 MPa to 40 MPa can be applied in this set-up.

For measurements at elevated temperatures a heating jacket can be used around the autoclave. This allows measuring of permeability at temperatures up to 180 °C.

Two types of pumps are available to generate the elevated pressure inside the autoclave. First, a HPLC pump (Merck-Hitachi L6200A) was used, later on a syringe pump (Teledyne ISCO 265D). The HPLC pump can only increase the pressure, which is mostly sufficient for measurements using gas. But when a single measurement requires a long time (temperature changing in the lab) or when working at elevated temperature a pump is required which can also reduce the pressure. In these case a syringe pump was used.

Samples measure about 30 mm in diameter and 30 mm to 50 mm in length (but only 10 mm to 20 mm in very low permeability rock samples). Samples are drilled from larger blocks or cores and cut to length. After drying at 60 °C for a day or longer depending on the permeability, samples were evacuated to pressures below 1 kPa. This is defined as dry condition.

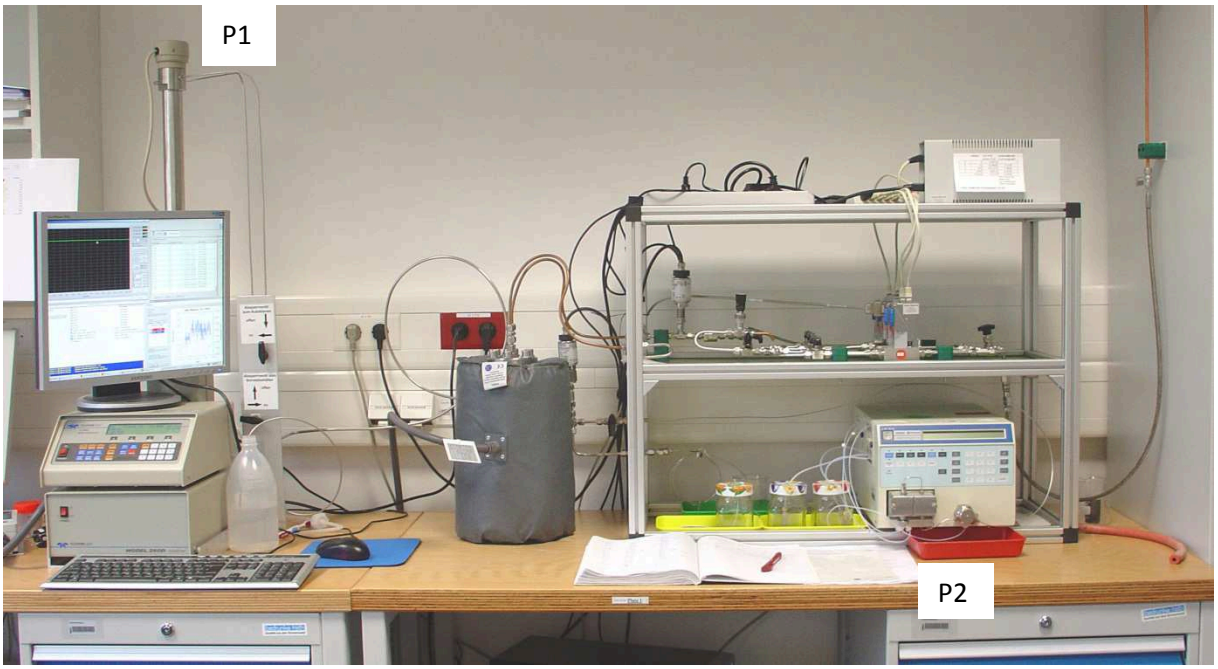

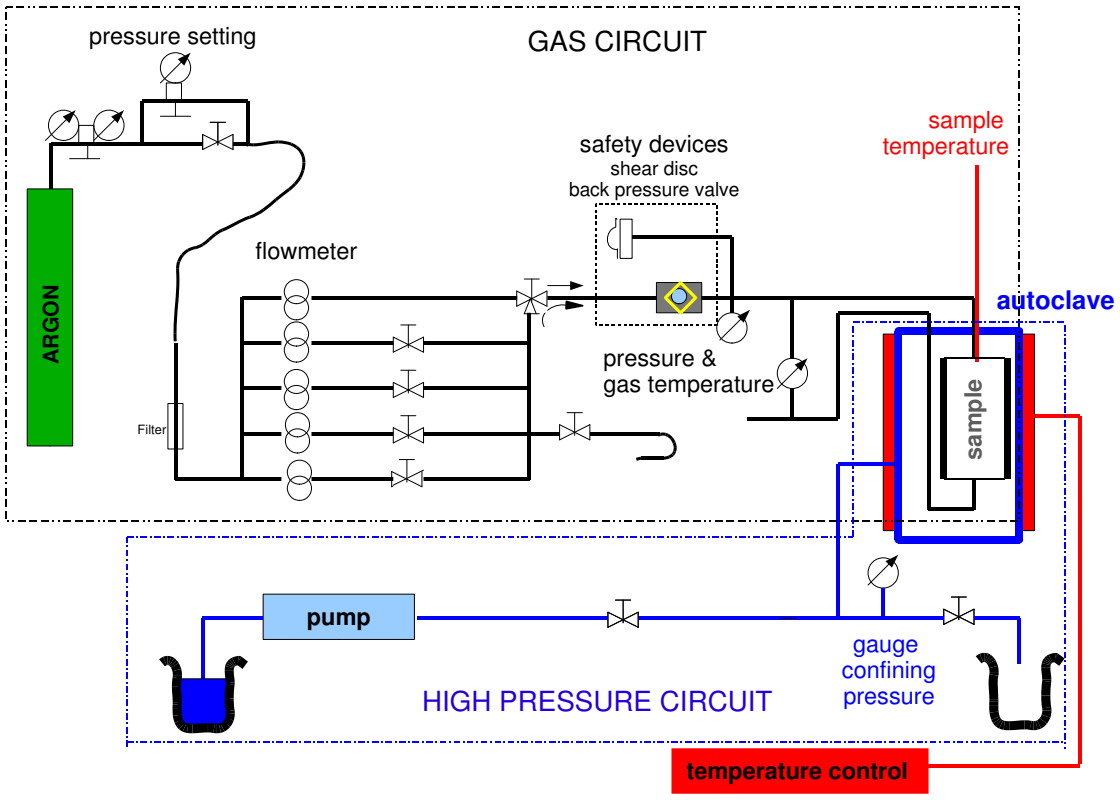

Fig. 1: The set-up for permeability measurements with Argon gas, photo and schematic diagram. The dark grey cylinder in the middle is the autoclave inside the heating mantle. Devices on lower left and right are two pumps, a syringe pump on left (P1) and a HPLC pump (P2).

2.2 Gas-permeability: Results

We illustrate results of permeability measurements using low-permeability rocks. These little permeable cores from boreholes in Northern Germany were studied for a third-party funded project. The plugs were drilled perpendicular to the core axis. Layers parallel to the sample axis are clearly visible in at least some samples. In anisotropic samples this is usually the direction of highest permeability, because low permeability layers are of less influence.

In these experiments, we increase the confining pressure in steps from 3 MPa to 30 MPa (30 bar to 300 bar). In each case, this pressure is applied for approx. ½ day only during the measurement. At each of these confining pressure steps the flow measurement was performed at gas pressures of around 0,1 MPa to 1 MPa (1 to 10 bar). The Klinkenberg method (e.g. Schön 1996) was used for calculating the intrinsic permeability, independent from fluid properties. Each gas pressure step is applied until gas pressure and flow-rate are constant. For one sample, this required about 4 days. Figure 2 shows the results of these measurements.

The Klinkenberg slip factor b (Eq. 2) is a further value to determine. The double logarithmic diagram of slip factor versus permeability (Fig. 3) shows the expected trend for a multitude of rocks also found in literature (e.g. Tanikawa & Shimamoto 2009): decreasing slip factors with permeability. We also obtain a decrease of permeability with pressure. As a result, the slip factor b also increases with confining pressure.

Pressures of 0.1 MPa (1 bar) are prefered for comparing rock permeability at elevated confining pressure with measurements at ambient pressure. Many authors describe the relationship between permeability k of rock samples and confining pressure p_c by a logarithmic function $\log k = f(p_c)$ (e.g. Schön 1996). For low permeability sandstones Kilmer et al (1987) found the relationship $\log k = f(\log p_c)$. Our measurements are described better by $k = f(\log p_c)$ (Fig. 4 & 5). This enables extrapolating measurements to ambient pressure for comparison with other data measured at this pressure (Nuclear magnetic resonance (NMR) data, porosity).

The depressurization of cores from some tens of MPa in the deep underground to surface pressure creates additional cracks in the rock. In the laboratory they partially close with confining pressure resulting in a decreased permeability. But this needs time, in the case shown in fig. 6 15 hours for a permeability decrease of 7 %. Suggestions in literature are waiting for a day or more with measuring after increasing the confining pressure.

Generally, for samples with permeabilities well below 10^{-15} m^2 the outflow pressure may be at atmospheric pressure and only the pressure at the in-flow needs to be measured.

Non-Darcy flow was noticed already at low input pressures for high permeability samples. To avoid non-Darcy flow for these samples, the measurement with gas required back-pressure, i.e. elevated pressure at the outflow side ensuring sufficiently high mean gas pressure inside the sample. Fig. 8 shows results of such measurements for a sample of Gildehauser Sandstone, a high permeable rocks with a permeability of 10^{-12} m^2. But also with back-pressure, non-Darcy flow occurred in this measurement indicated by the non-linear part of the curve at high differential pressure. Liquids with a viscosity 50 to 100 times higher than gas may solve this problem.

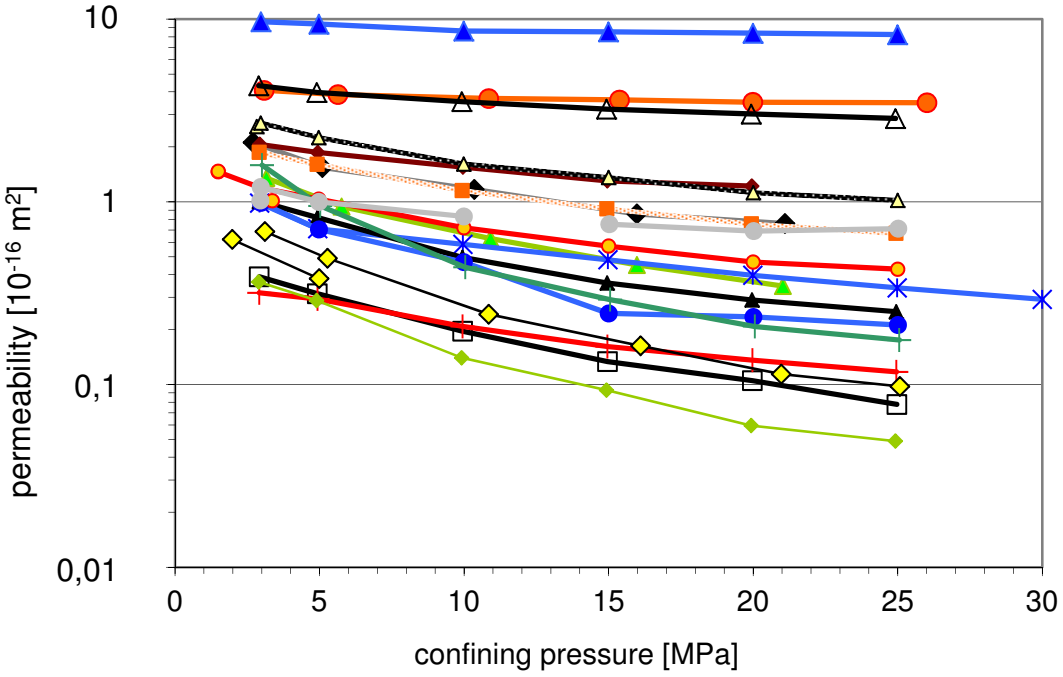

Fig. 2: Permeability vs. confining pressure for 17 predominantly low permeability rock cores. Permeability ranges from $5x10^{-18}$ m^2 to 10^{-15} m^2.

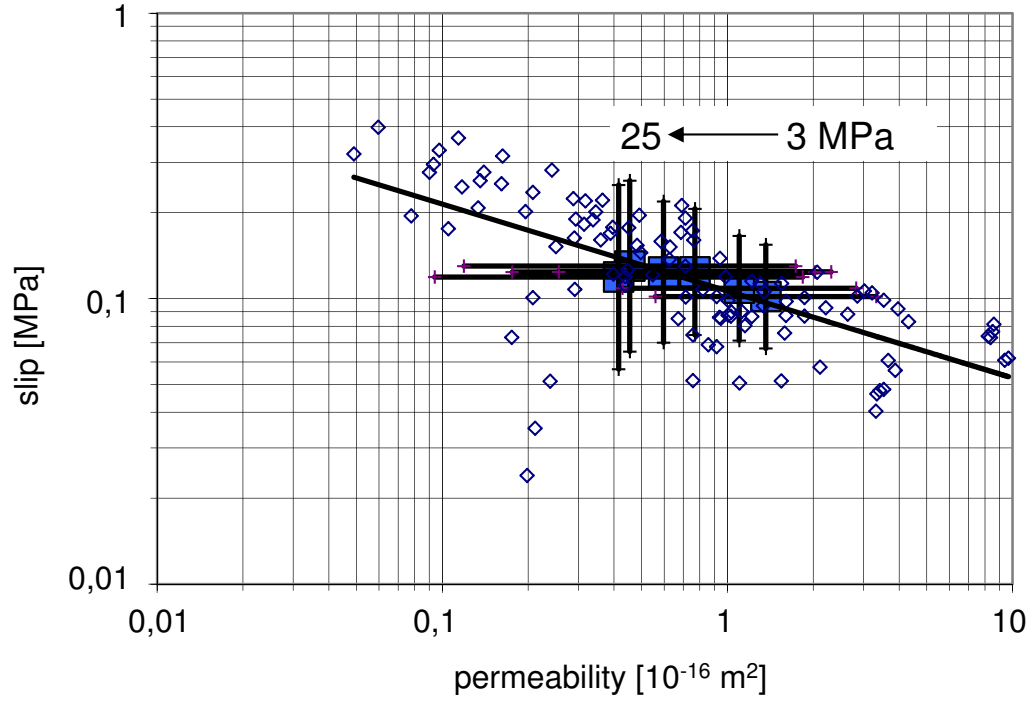

Fig. 3: Slip calculated after Klinkenberg for a multitude of samples with different confining pressures (diamonds). Blue squares are mean values (± standard deviation) for the confining pressures steps from 3 MPa to 25 MPa (all samples from Fig. 2)

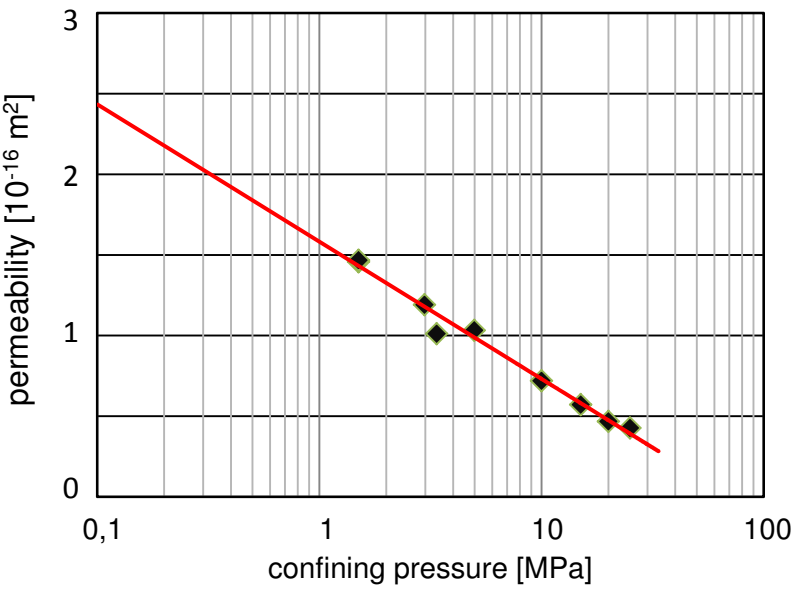

Fig. 4: Permeability of low porosity rocks is best described by semi-logarithmic linear relationship of permeability and confining pressure.

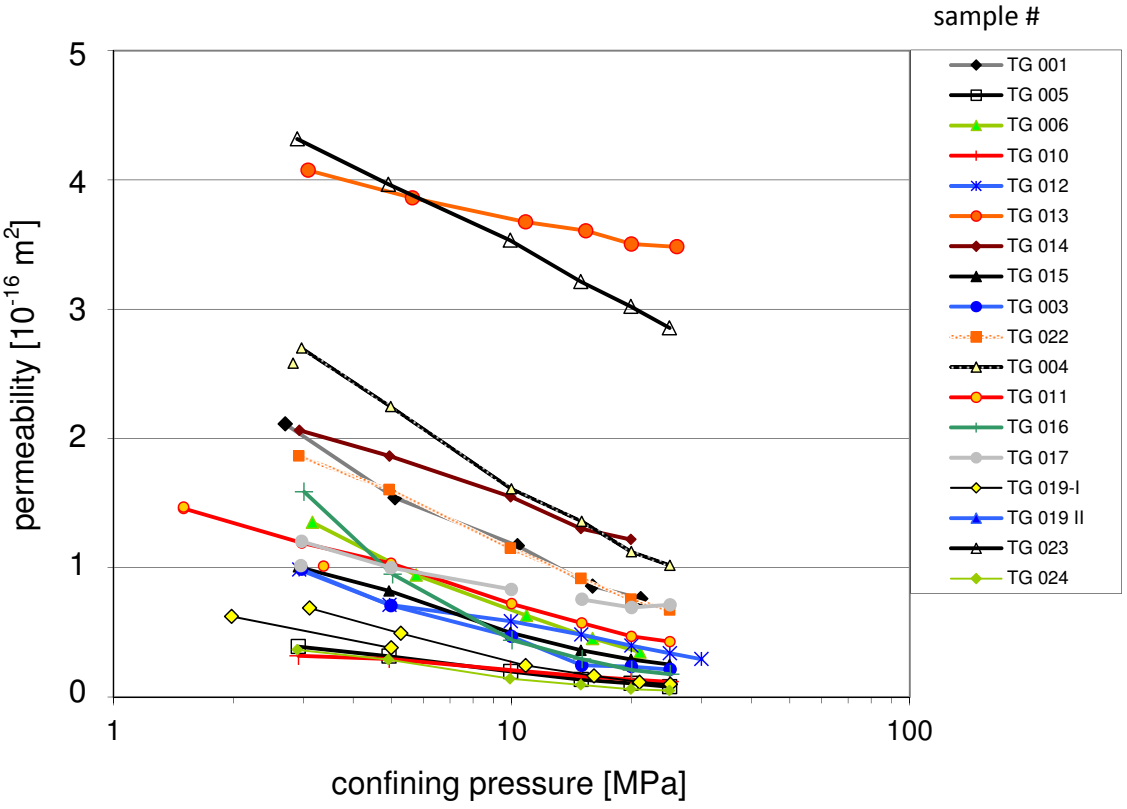

Fig. 5: Permeabilities from figure 2 plotted versus logarithmic pressure, indicating a linear relationship.

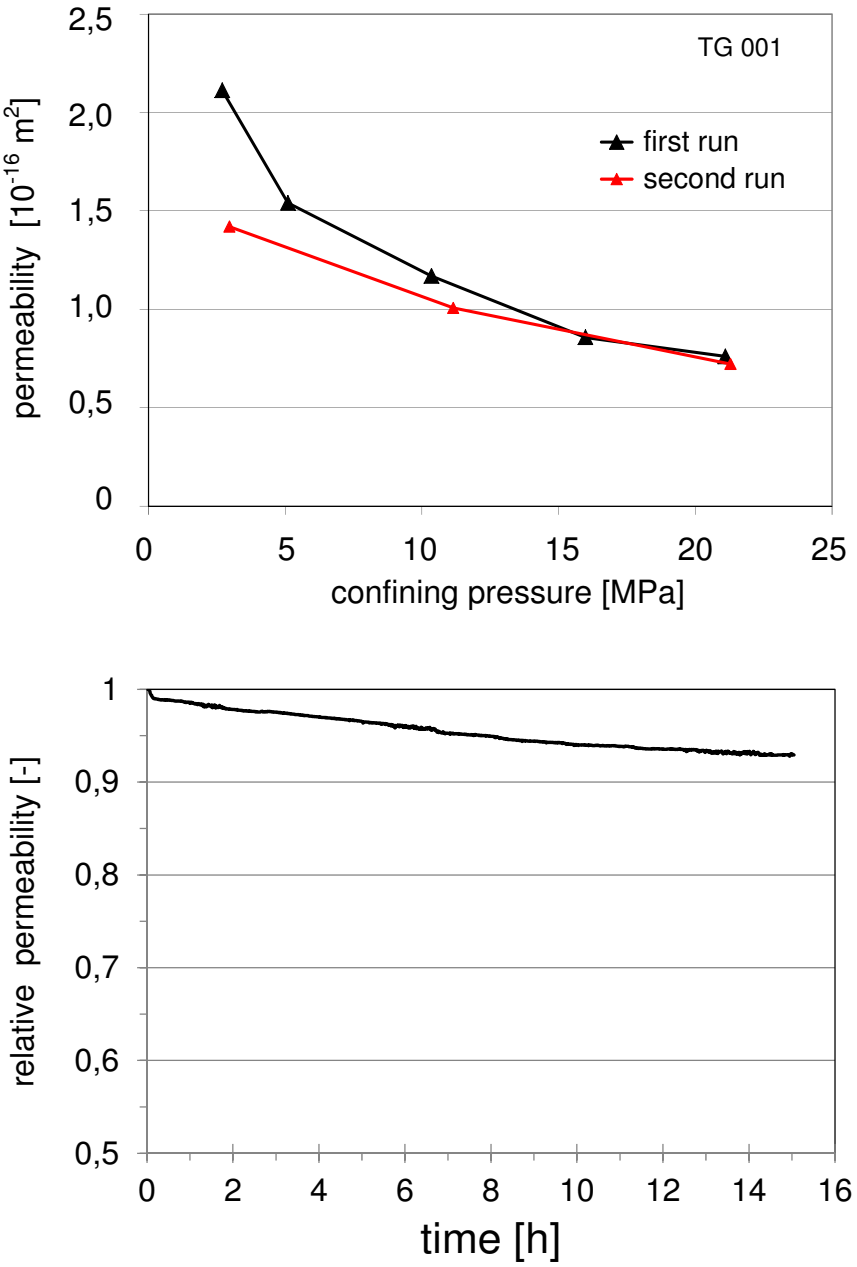

Fig. 6: Permeability measured with Argon on cores from greater depth. Cracks resulting from depressurization close only slowly with increasing confining pressure. In lower graph, the pressure was increased at time zero from 0 MPa to 1.9 MPa. During the next 15 hours, permeability decreased by 7% (sample TG 014). This is also visible on the upper graph when measuring the pressure dependence twice (TG 001). After the first run, the confining pressure was released to 3 MPa not to zero. On next day, the second run starts at lower permeability (red line).

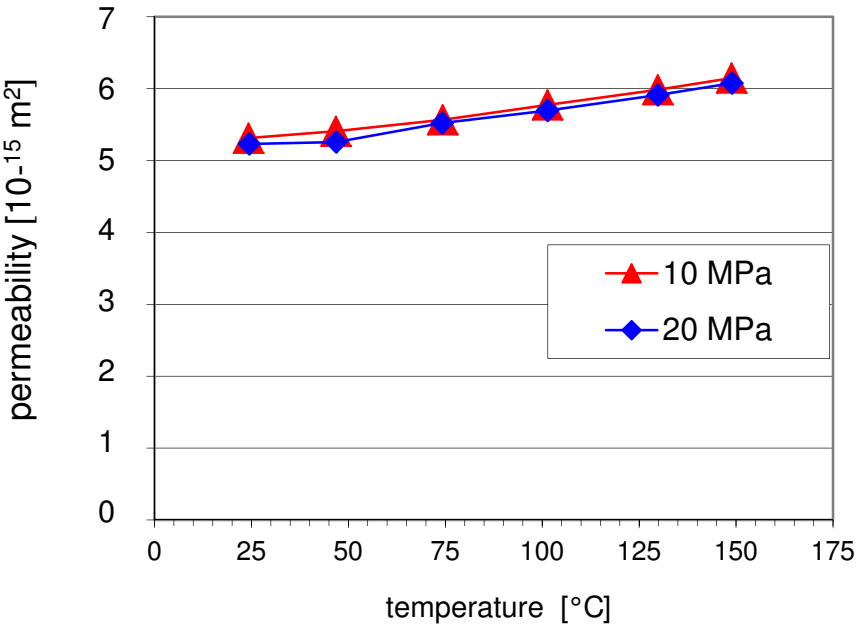

Fig. 7: Permeability of Obernkirchener Sandstone (sample G4A) at temperatures from 25 °C to 150 °C at 10 MPa and 20 MPa confining pressure. This sample from a quarry shows only a very small decrease in permeability with the two measured series at different confining pressure indicated by the negligible difference.

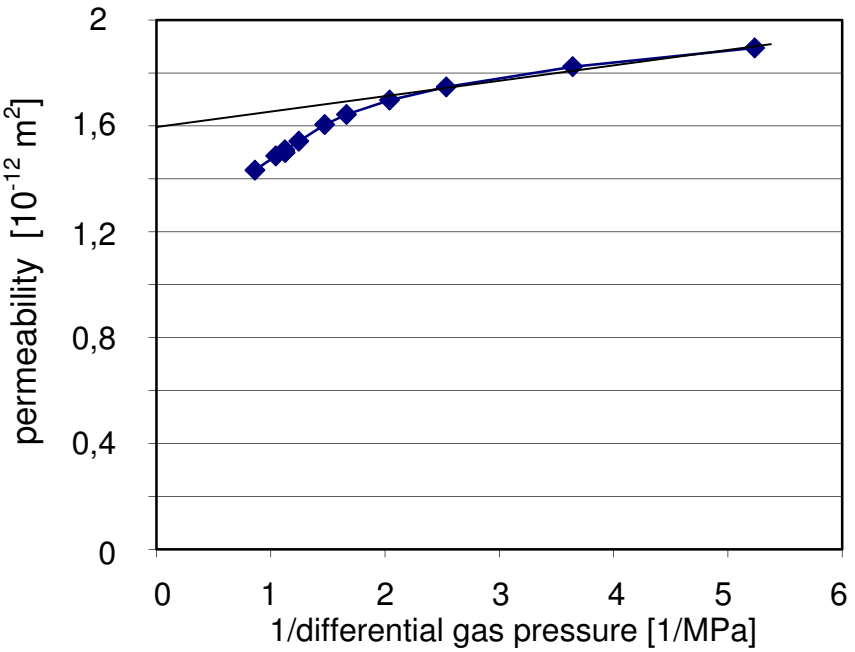

Fig. 8: Klinkenberg plot for a high permeability sample (Gildehauser Sandstone). Non-Darcy flow is indicated in the left part of the plot, at high gas pressure.

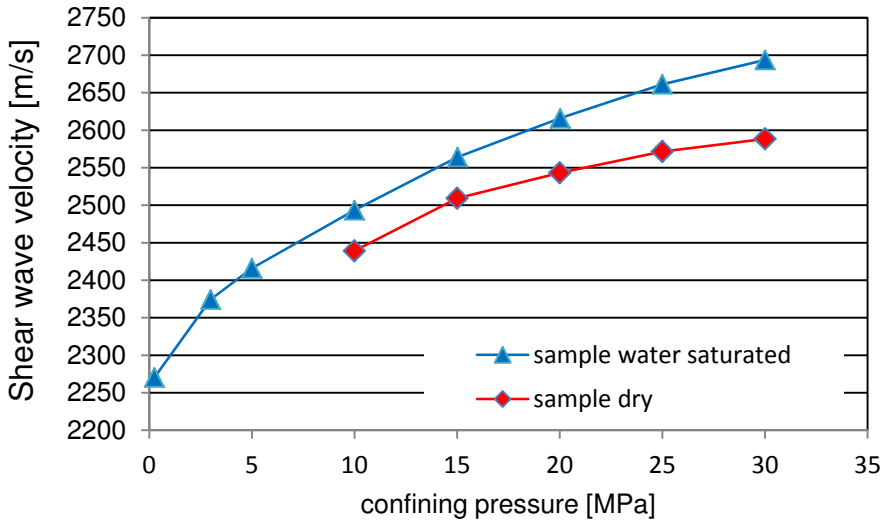

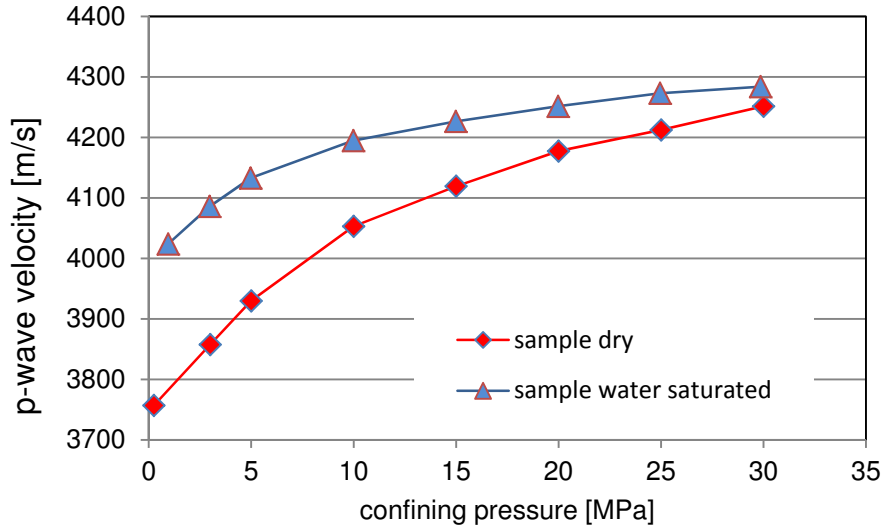

Fig. 9: Ultrasonic shear wave velocity (upper graph) and compressional (p-) wave velocity (middle graph) of Obernkirchener Sandstone in dry (red) and saturated condition (blue) for confining pressures of up to 30 MPa.

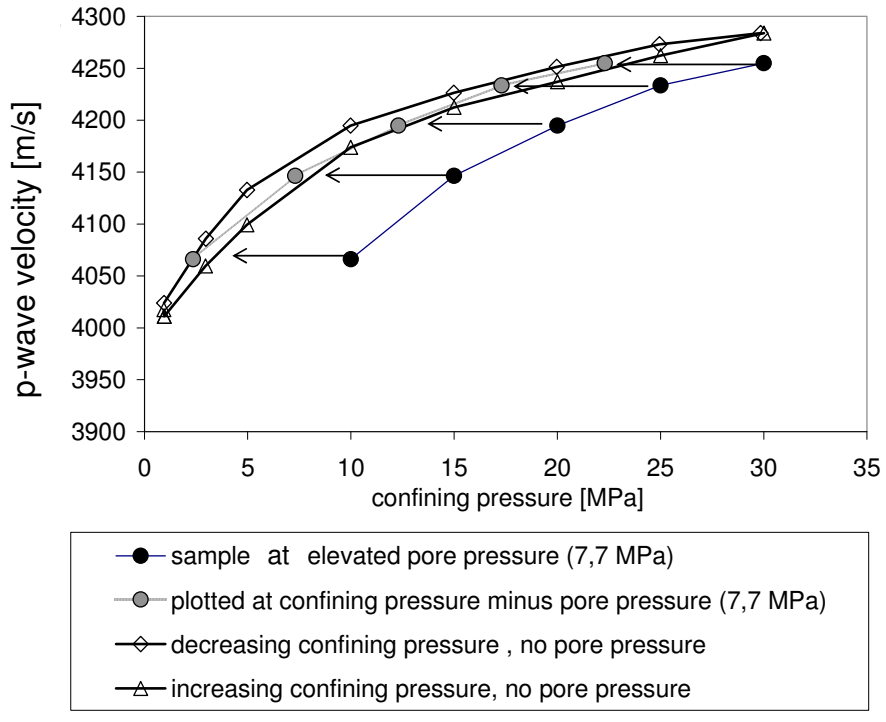

Fig. 10: The same sample of Obernkirchener Sandstone as in figure 9 saturated with water but at elevated pore pressure.

2.3 Gas-permeability at elevated temperature

A heating jacket around the autoclave allows measuring permeability at temperatures of up to 180 °C. Shrinkable tubes are used for blocking gas or fluid flow along the cylinder mantle of the sample. While they are stable at temperatures below 80 °C, they are not stable at high temperatures. A 1 mm thick lead foil was used instead, soldered at the contact line. Lead foil is soft enough so that the confining pressure closes all possible flow paths along the surface. Figure 7 displays data from such an experiment. There is only a minor effect of temperature.

3. Propagation of elastic waves: ultrasonic velocities

Measuring ultrasonic wave velocities requires a different sample holder in the autoclave. The waves propagate along the sample axis. One ultrasonic source is encapsulated and put inside the autoclave and two receivers outside. Measuring the propagation of waves restricts the frequencies of the ultrasonic waves as the wavelength need to significantly smaller than the sample dimensions. The main frequencies of our ultrasonic wave transducer are between some hundred kHz and 2 MHz, resulting in wavelengths in the mm-range, depending on the wave velocities of the rock samples.

As receivers we use one p-wave and one s-wave piezo-electric transducer. A shear wave transducer is a source of both compressional (p) and shear (s) waves. Beside s-waves, the s-wave piezoelectric transducer produces also p-waves at smaller amplitude . Because p-waves are faster than s-waves they can be detected also at small amplitudes.

Wavelengths in the mm-range lie often in the size of laminations. If a lamination is in the direction of the cylinder axis interference may be a problem for identifying the first arrival of s-waves.

Measurements can be also performed at elevated pore pressure as long as it is below the confining pressure. For pumping fluid through the sample the experimental set-up has tubes from outside into the sample.

Figure 9 shows typical measurements of p- and s-wave velocity in a sandstone at dry and saturated conditions and different confining pressures. Figure 10 demonstrates the effect of elevated pore pressure. The pore pressure reduces the effective stress yielding velocities at an effective confining pressure equal to the difference between confining pressure and pore pressure. Absorption or attenuation of elastic waves results in a reduction of amplitude and modified frequency spectrum. Either, amplitude or spectrum, may be used for calculating the attenuation. Obtaining an absolute value requires information on the transmitted waves. Usually the transmitted wave through a sample of comparable dimensions and known attenuation is used in the lab an aluminum sample with negligible attenuation. Different pressure- and saturation-dependent transmission coefficients between pistons (steel cylinders with grooves for fluid injection) and rock or reference sample result in insufficient by defined characteristics of decreasing amplitudes and spectrum. Isolated wavelets or at least the first wave trains are necessary for determining a relative changing of attenuation. Homogeneous samples of specific velocity and dimensions may satisfy these conditions. But the unknowns are the transmission coefficients between pistons and sample and their dependency on

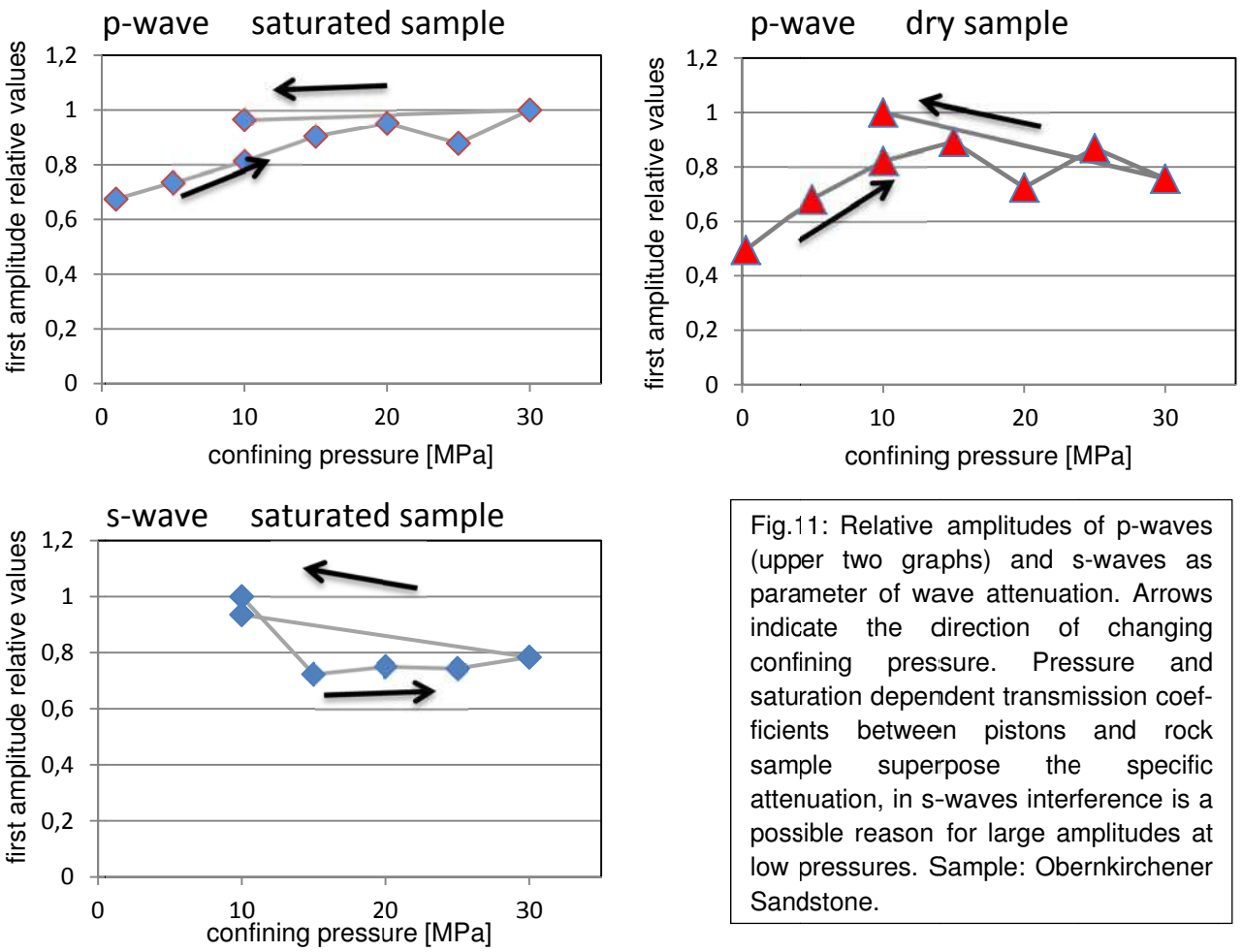

Fig.11: Relative amplitudes of p-waves (upper two graphs) and s-waves as parameter of wave attenuation. Arrows indicate the direction of changing confining pressure. Pressure and saturation dependent transmission coefficients between pistons and rock sample superpose the specific attenuation, in s-waves interference is a possible reason for large amplitudes at low pressures. Sample: Obernkirchener Sandstone.

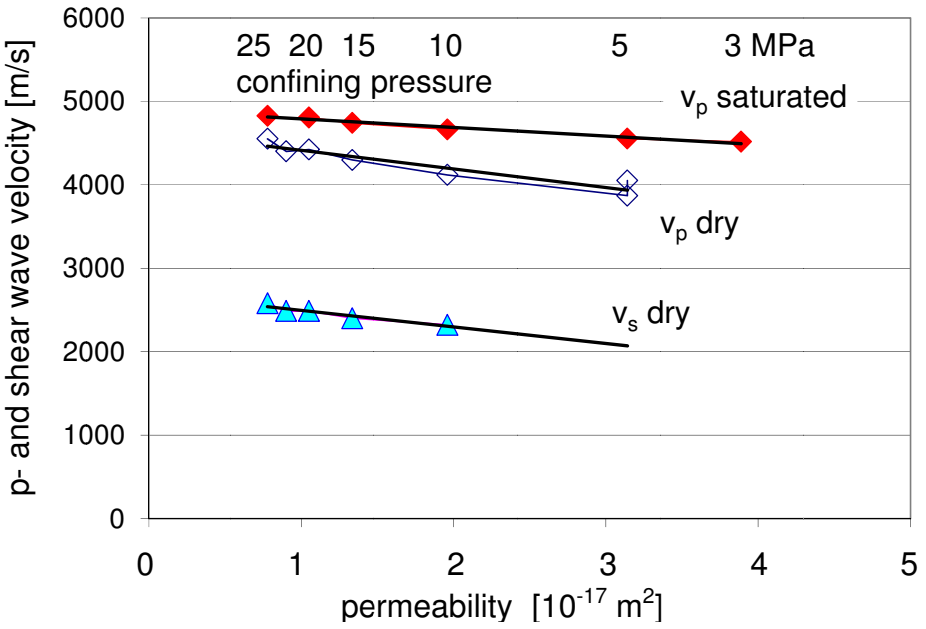

Fig. 12: Sample TG 005 from a deep drilling. Compressional- (v_p) as well as shear wave velocity (v_s) is increasing with increasing confining pressure (right to left) for dry and saturated sample whereas the permeability (fig. 2 and 5) is decreasing with increasing confining pressure. This is coherent: with increasing pressure the cracks are closed resulting in less permeability and the rock becomes more compact resulting is a higher velocity.

pressure and saturation. Measuring of the above-mentioned low permeability rock sample yielded no trustworthy rock-specific amplitude reduction. Results are better for the homogeneous Obernkirchener Sandstone (Fig. 11). The pressure-dependent reduction of attenuation of p-waves for a dry sample is between 5 and 10 times larger than measured an other samples of Obernkirchener Sandstone with a more sophisticated set-up (Schütt 1992).

Only a minor change in velocities is observed for a permeability decrease by a factor of 5 in the rock sample TG 005 (Fig. 12).

4. Permeability measured with liquids

Measurements with gas are the usually used for determining fluid-independent permeabilities values of natural rocks. However, the most frequent pore fluid in the underground is water. Values calculated from gas measurements in nearly all cases are larger than those measured with water. Therefore these values need to be known. At first, we thought to accelerate also the measurements, no Klinkenberg correction has to be made. As following experiments show, other effects are contrary to acceleration. Water is no inert medium, chemical and physical reactions occur in the pore-space. For example, there are often great differences between fresh and saline water (see detailed list in Schopper 1982; Tanikawa & Shimamoto 2008).

To avoid non-Darcy flow (see fig. 8) high permeable samples are measured best using fluid of higher viscosity than gas.

4.1 Liquid-permeability: Methods, measuring set-up

The experimental set-up used for permeability measurements with Argon gas was modified for water. As in the case of gas flow the pressure at the inflow was measured with a digital pressure transducer. The flow was not measured itself but the pump could be set and this value was taken for calculation. Two types of pump were available. First a syringe pump (Teledyne ISCO 265D, later also 65D) was used, this type is working like a syringe and shows only a small pulsation during a wide range of flow rates. The volume is limited to 265 ml or 65 ml. After emptying the cylinder, the pump has to be filled again, manually. This flow interruption sometimes prevents recording a continuous permeability curve. In this case, the HPLC pump proved useful. This type of pump works continuously like a single cylinder engine. A second anti-cyclical working cylinder is used to suppress pulsations but the pressure variation is still clearly visible, in particular for low flow rates resulting from low pump rotation speeds. The pressure may change by ±15 % due to changing flow, but we use a mean value. We cannot exclude that this pressure pulsation has an effect on the flow through the rock and may promote or obstruct some of the observed effects.

The fluid which passed through the sample was collected in a beaker glass and weighted each time after the flow settings had been changed. The flow calculated from this total flow-through agreed well with the pump settings (difference mostly < 0.1 %).

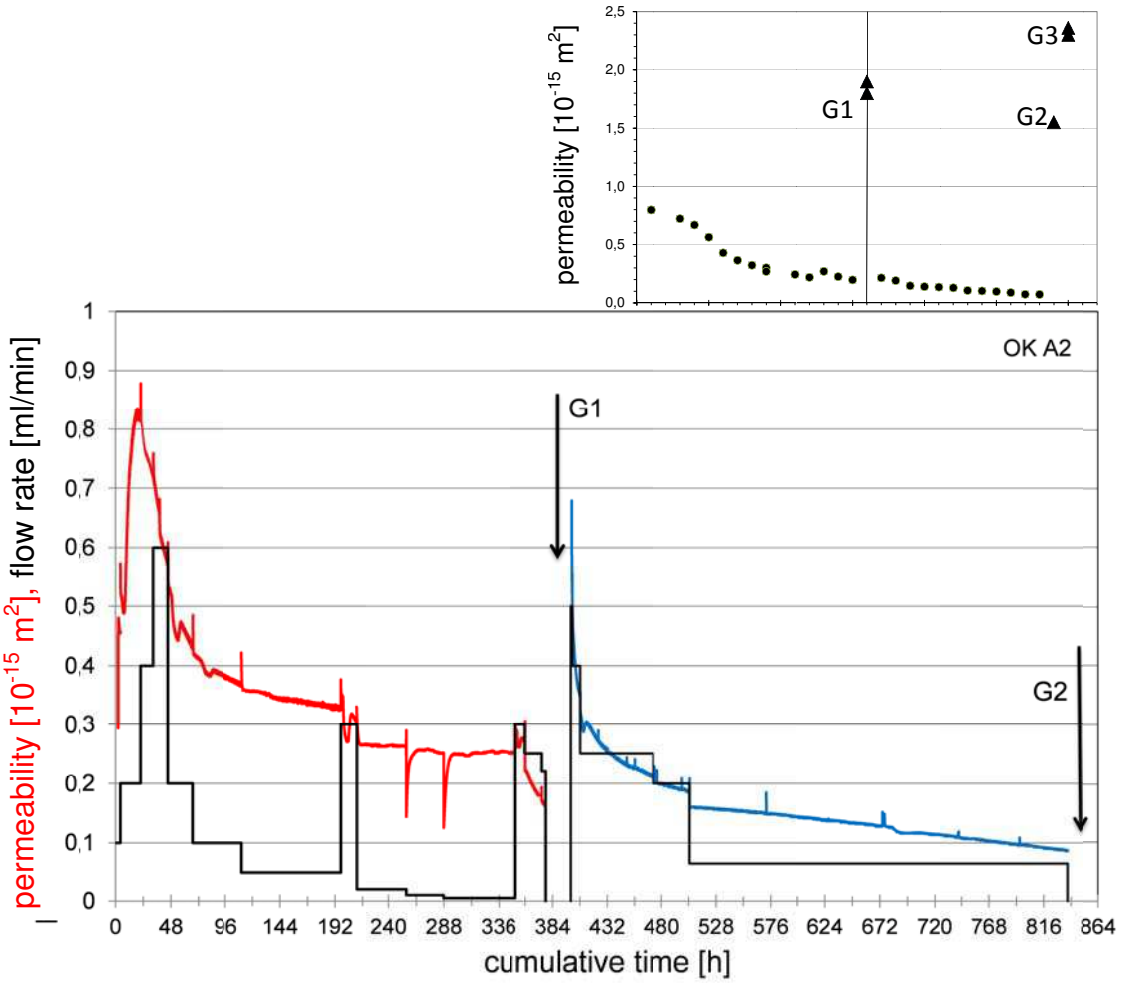

Fig. 13: Permeability of a sample of Obernkirchener Sandstone (OK A2) measured with tap water as fluid. The figure is a combination of piecewise measurements with a syringe pump. At G1 and G2 the sample was dried and measurements of permeability are done with gas. After G2 the sample was cleaned with hydrogen-peroxide and measured with Argon a second time G3. The values of the measurements with gas (G1, G2, G3) are plotted relative to the mean values of both runs with water in the small graph above.

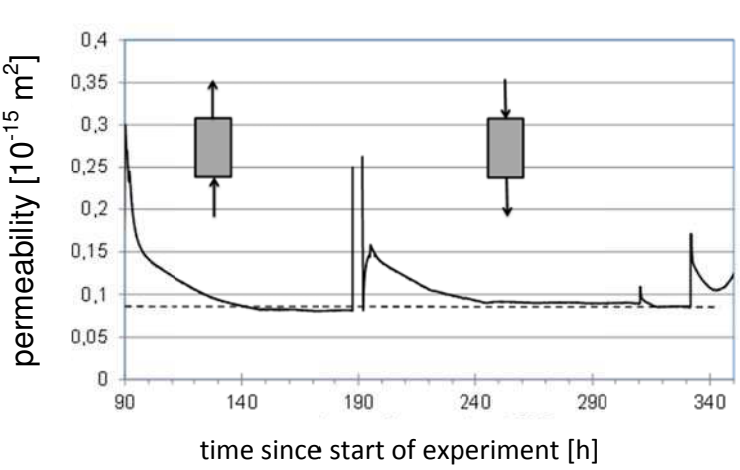

Fig. 14: Changing of water flow direction through the sample. After pressure build up the permeability was the same in both flow directions.

For these series of measurements we used a pressure transducer with an accuracy of 0.05 % of the end value. First, a range of up to 1 MPa was used, but after exceeding the maximum pressure and damaging the transducer others with a maximum pressure of 3 MPa were used. This increases the range of error in the low pressure range especially far below 0.1 MPa.

Permeability is calculated again according to Darcy's law. As the viscosity of the fluid depends on temperature, this has to be considered during the analysis. With a thermocouple the fluid temperature is measured in the tube at outflow side of the sample inside the autoclave. A second thermocouple was inside the pressure transducer at the inflow side. These data are all digitally registered at the PC. The great mass and heat capacity of the autoclave and the water inside damps the thermal fluctuation in the laboratory.

For an experiment, the sample was saturated in a vacuum chamber with tap water, demineralized water or demineralized water additionally boiled for more than one hour. Alternatively, demineralized water was disinfected with ultrasonic equipment (Bandelin Sonorex Digitec, Ultrasonic frequency 35 kHz, 80 W_{eff}). When using a sample a second time which was contaminated by micro-organisms, it is necessary to clean the samples from organics. This was done with hydrogen peroxide (H_2O_2), a strong oxidant and bactericide. In this case, the dry sample was put into a beaker glass with H_2O_2 and evacuated for a short time. It was kept in this fluid under low pressure until no gas bubbles were visible on the sample surface. H_2O_2 was added to water in low concentration (>< 3%) in one test series.

Some samples were measured with saline water (NaCl). The concentration was defined by the electrical conductivity.

Additionally isopropyl alcohol was used as pore fluid, as it acts as a bactericide without the high electrical dipole moment of water.

With simple commercial agar plates (Bode Dip Slides Combi) for detecting bacteria, fungi and yeast we looked for micro-organism in the water. This is only a rough estimation, yielding an order of magnitude at best. Only a fraction of the bacteria species - the most important for health care - can be verified this way, much more cannot be bred. Sampling was done in the water before the pump (storage vessel), from the tube behind the pump (autoclave inflow) and the outflow behind the sample. Samples are taken at different conditions: the water from outflow are between 1 day (high flow rate) and 4 days (low flow rate) exposed to air in a beaker glass before getting enough fluid for wetting the agar plates. During this time the number of bacteria could increase in the laboratory at temperatures above 22°C. Not the single size of the colonies, the density is the indicator, this is important for interpretation of figure 20.

4.2 Liquid-permeability: Experimental results

In a first experiment, we used a sample of fine-grain, clean quartz sandstone (Obernkirchener Sandstone). A syringe pump delivered a constant flow of water, in the first experimental series tap water. Tap water contains only very few micro-organisms and minerals by law (upper limit) but not quantified in detail. The confining pressure was held constant at 3 MPa. The fluid pressure difference was measured between in- and outflow. But instead constant

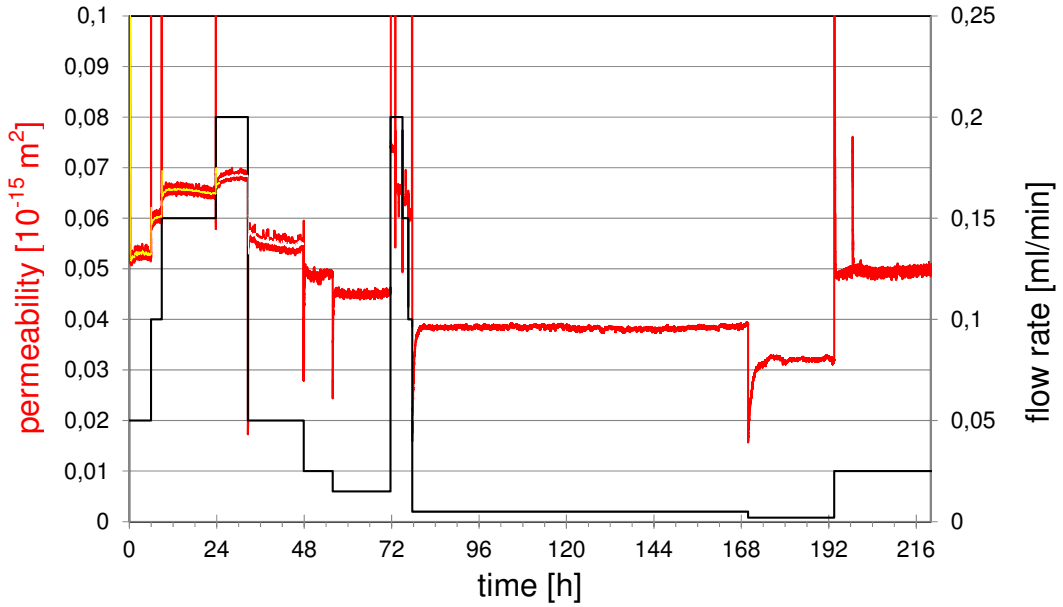

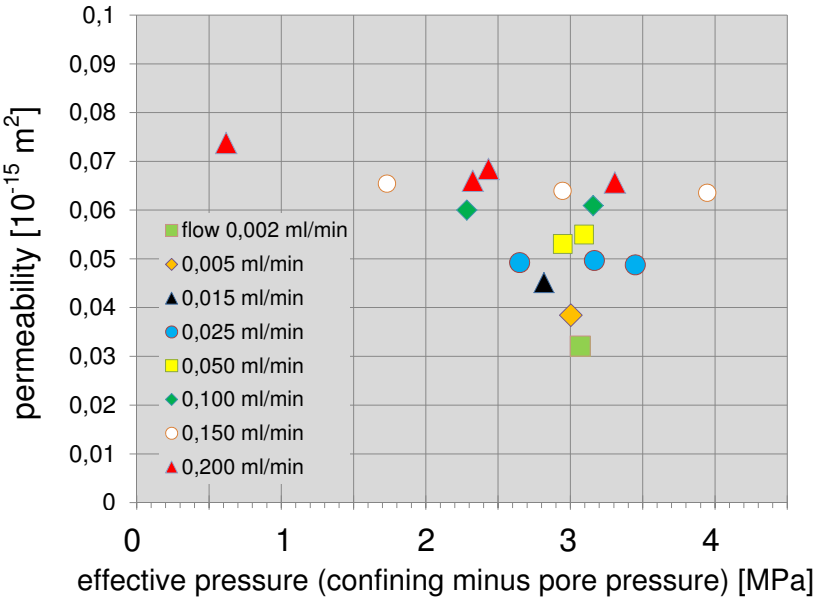

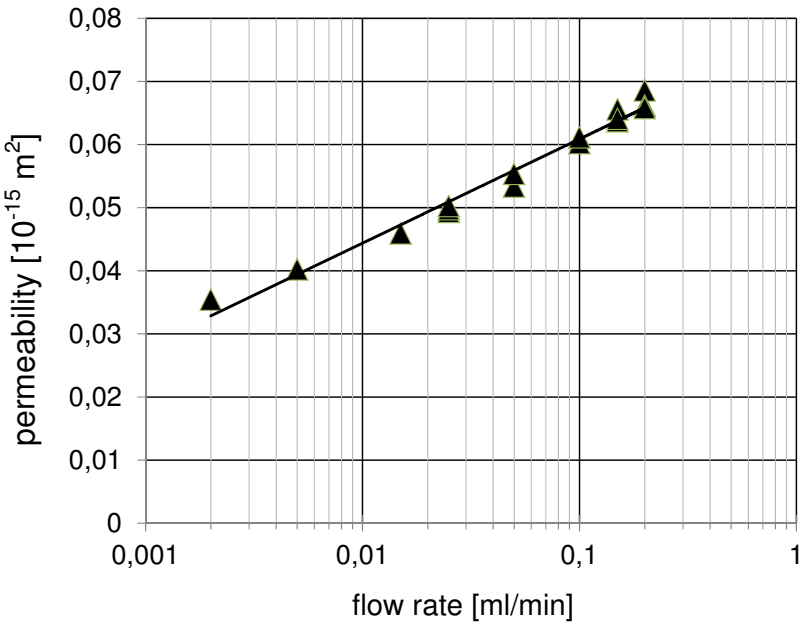

Fig. 15: Correlation between flow rate of water and permeability (sample Obernkirchener Sandstone OK B1_IV). Top the measured time series. After a long time of fluid flow through the sample only a minor decrease is visible in this time span (less than 1 %).

Centre: Permeability data for eight values of flow rate. In a broad range of effective pressure, permeability is independent of pressure. For excluding any time dependencies, measurements are not performed in systematically increasing or decreasing order.

Bottom: Permeability versus flow rate. Permeability is increasing with flow.

pressure at constant flow rate, a slight increase of pressure is visible in all data of each pump run (≤ 265 ml). Also, on longer time scale (not only in the range of hours), the ratio of flow and pressure was not constant. Figure 13 shows the resulting variation of permeability with time. On this long time scale, more than a month of measurements, there is a continuous decrease of permeability. During the last part of the experiment the pressure variation was small. Only the long-term trend indicates that no steady state was reached. This experiment was stopped a first time after 3 weeks (383 hours cumulative flow). The sample was dried and permeability was measured with Argon gas. For confirming or excluding a partially blockage through micro-particles as reason, two measurements were performed with opposite flow-directions yielding permeabilities of $1.8*10^{-15}$ m^2 and $1.9*10^{-15}$ m^2. Within the error margins, the values are the same in both directions, but permeabilities clearly larger than with water. These gas measurements were followed by another 3 weeks of water flow through the sample. After a short transition period, the next trend follows seamlessly. Altogether, about 5 L of water were pumped through the sample (17 % porosity), more than 1000 times the pore volume. At the end, a gas measurement yielded a permeability of $1.55*10^{-15}$ m^2. After cleaning with hydrogen peroxide, permeability increased to $2.3*10^{-15}$ m^2. This is interpreted as a reduction of permeability by a biofilm and later the destruction of the microorganism with H_2O_2. A further run was done to measure the flow of water in both directions. As before with gas, this yielded nearly the same values for both directions (Fig. 14).

After the first experiment with tap water, others were performed with demineralized water, demineralized water additionally treated in an ultrasonic bath, and also additionally boiled for more than one hour. In all these experiments, permeability decreased clearly with time.

Permeability should be independent of flow rate over a wide range. This is not the case here. There is a distinct dependence on flow rate (Fig. 15 bottom), when permeability is at low and time dependence is of minor importance after a long experiment duration. During the long time measurements the confining pressure was kept constant to 3 MPa in majority of experiments, that means with decreasing permeability the effective pressure at the sample matrix was decreasing because of increasing pore pressure. The most used Obernkirchener Sandstone samples are from a quarry, no decompression takes place and therefore no decompression fractures occurred. This results e.g. in a negligible pressure dependence of permeability measured with gas in this pressure range. This is true for water. We set here the confining pressure such, that the effective pressure (confining pressure minus inflow pressure) on the matrix was always the same beside the usual constant confining pressure (Fig. 15 centre). A wide range of effective pressure yielded the same permeabilities. The result is nearly independent if the measurements are in descending, ascending, or in mixed order - the flow dependence of permeability is reversible. One possible cause for this assumption may be pressure dependent resistance elements in the water saturated pore space. Biofilms extending into the flow channels in form of pillars or mushroom-like structures may form such elements.

With a different rock type, a sample from a deep borehole we used saline water. Again we observed a decrease of permeability and a flow-dependent permeability (Fig. 16).

In another experiment isopropyl alcohol (C_3H_8O) was used as measuring fluid. This should exclude the growth of most micro-organisms. Because of the small electrical dipole moment,

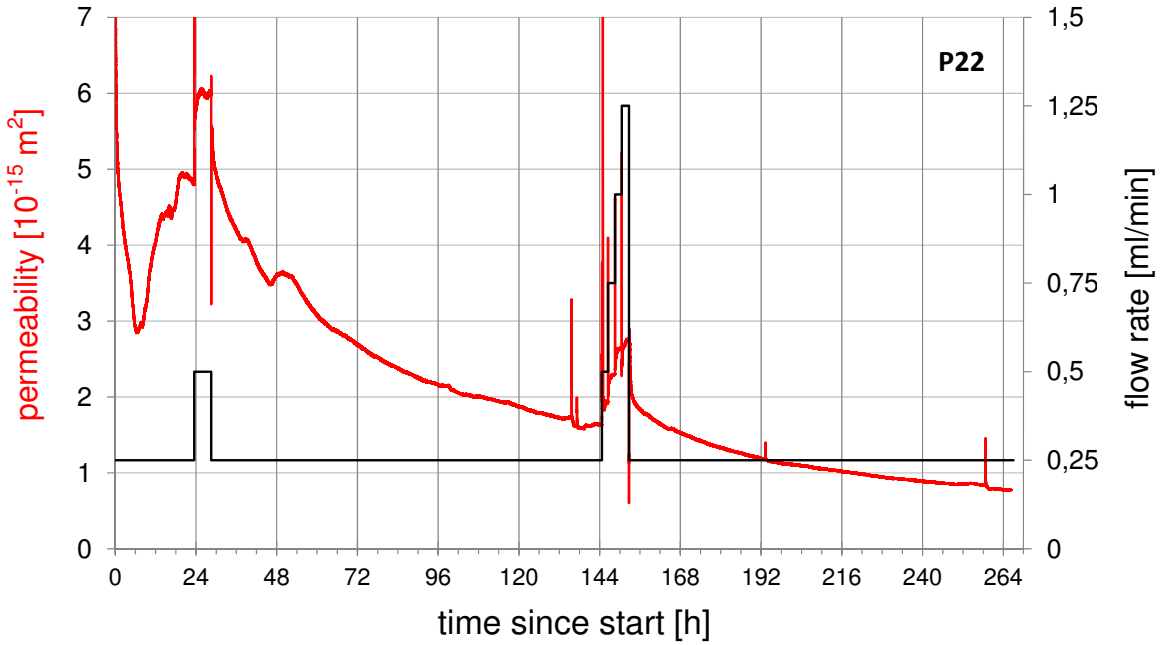

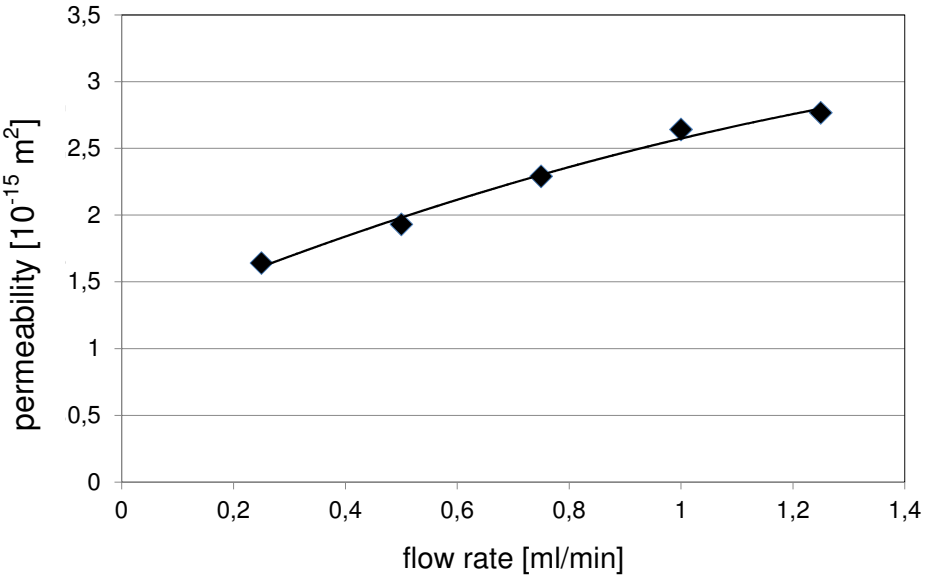

Fig. 16: Permeability determination of sample P22 from a deep borehole. The original highly saline pore water was substituted by a water of lower salinity (2 mS/cm). Also in this case a drastic permeability reduction is visible. Permeability depends on flow, as in Obernkirchener Sandstone permeability increases with flow rate.

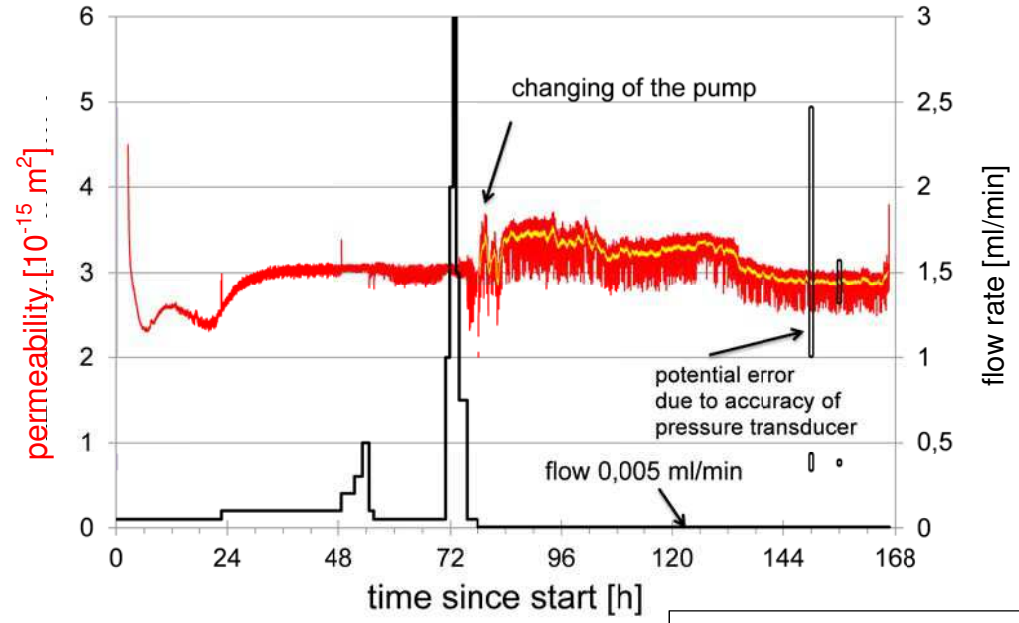

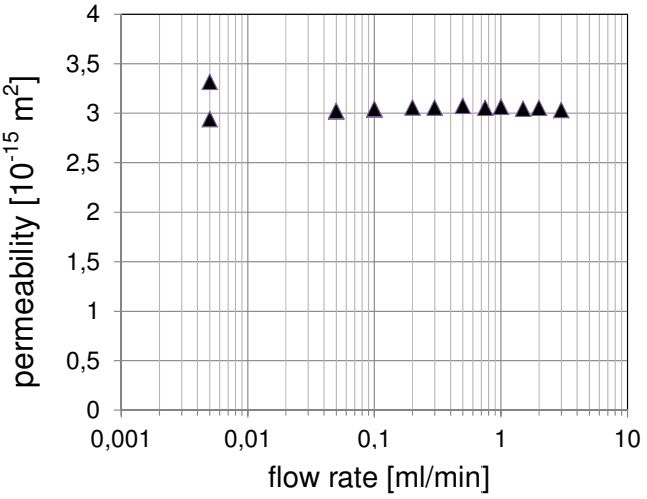

Fig. 17: Isopropyl alcohol as fluid. After the starting phase of approx. 32 h the permeability is independent of flow rate. After 78 hours the pump was changed, because of extremely small flow rate. It needs a long time to establish a constant flow. The two dots in the lower graph left are the mean values of the time period 83 h to 132 h and 132 h until the end. Altogether the permeability in this case is independent of flow rate. Sample Obernkirchener sandstone OK A14-A.

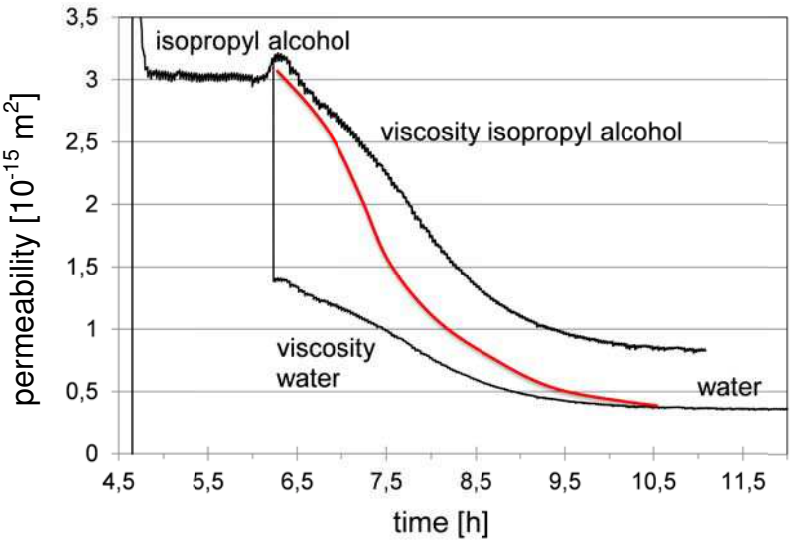

Fig. 18: The pore fluid at inflow was changed from isopropyl alcohol to water at 6 h. Four hours later at 10.5 h water was the dominant or only fluid. The real fluid composition in this transition zone is not known, permeability was calculated with viscosity of isopropyl alcohol (upper line) as well as with that of water (lower line). Something like the red curve drawn by hand should be the real transition function. Permeability for water is about 10 % of that for alcohol.

no important double layer developed as in the case of water at the inner surface of the pore space. Figure 17 shows, that after the starting phase permeability is independent of flow rate. This is an additional strong indicator that partial blocking of the flow path through particles is not the reason for decreasing permeability values.

When exchanging isopropyl alcohol by water we notice a strong decrease of permeability. Permeability in the transition section was calculated with viscosity of isopropyl alcohol and of water, because we do not know the time dependent composition inside the sample. This 80 % decrease reflected the effect of the double layer of water molecules at the internal surface, which constrained the flow (Fig. 18).

A decrease of permeability with decreasing fluid flow is unusual. Under normal conditions an increasing flow rate might lead to a change from laminar to turbulent flow where eddies decrease the permeability. As mentioned before permeability remains constant however when using for the same sample isopropyl alcohol as fluid (Fig. 17).

In the light of the above mentioned results, we inspect again another experiment. These data had not been used, partially because of the behaviour of the tested HPLC-pump could not really explained until now. Fig. 21 shows a series of measurements performed for testing this pump. The permeability curve is superimposed by a strong sawtooth signature. However in this case we obtained nearly time-independent permeabilities, but also with a dependence of flow-rate. This experiment differed in some details from the others:

1.) First, the sample already used in a previous experiment was saturated with hydrogen peroxide H_2O_2 and put into the ultrasonic bath. Then the sample was put into vacuum with fresh H_2O_2 and later cleaned with water. The dry sample was put into the sample holder, a vacuum pump was used, when pumping the first time outflow. Because of the sawtooth signature the experiment was stopped and started a second time after cleaning the sample once more hydrogen peroxide H_2O_2. This time, the sample was saturated with H_2O_2 when put into the sample holder. A vacuum pump was used at the outflow for a short time. But results did not change. After 4 days the test pump was exchanged against our usually used Merck-Hitachi pump because of the sawtooth in the pressure curve. In the following time we obtained the usual results with decreasing permeability without sawtooth signature. After changing again to the tested pump we obtained a nice trend without pulsation, but later again the sawtooth signature.

2) The sample was much more cleaned and therefore disinfected with the ultrasonic bath and hydrogen peroxide H_2O_2

3.) Short pieces of copper tubes are used which corroded. This tubes are not chemically inert against hydrogen peroxide.

4.) We realized later, that the demineralized water was possibly somewhat older and may be a bit older and a slimy layer could be seen at the bottom of the supply tank – most likely bacteria.

5.) Probably more importantly, the inflow filter at the test pump had a smaller mesh (2 µm instead of 10 µm). This filter was slimy when pumps were exchanged after a relatively short time of operation. But the size and therefore the inflow surface were really small compared to the other filters used. After noticing a clogging effect at the filter of the Merck-Hitachi pump the first time, we changed and cleaned the filter more often. Clogging of the filter until a specific underpressure could be a reason for the sawtooth signature.

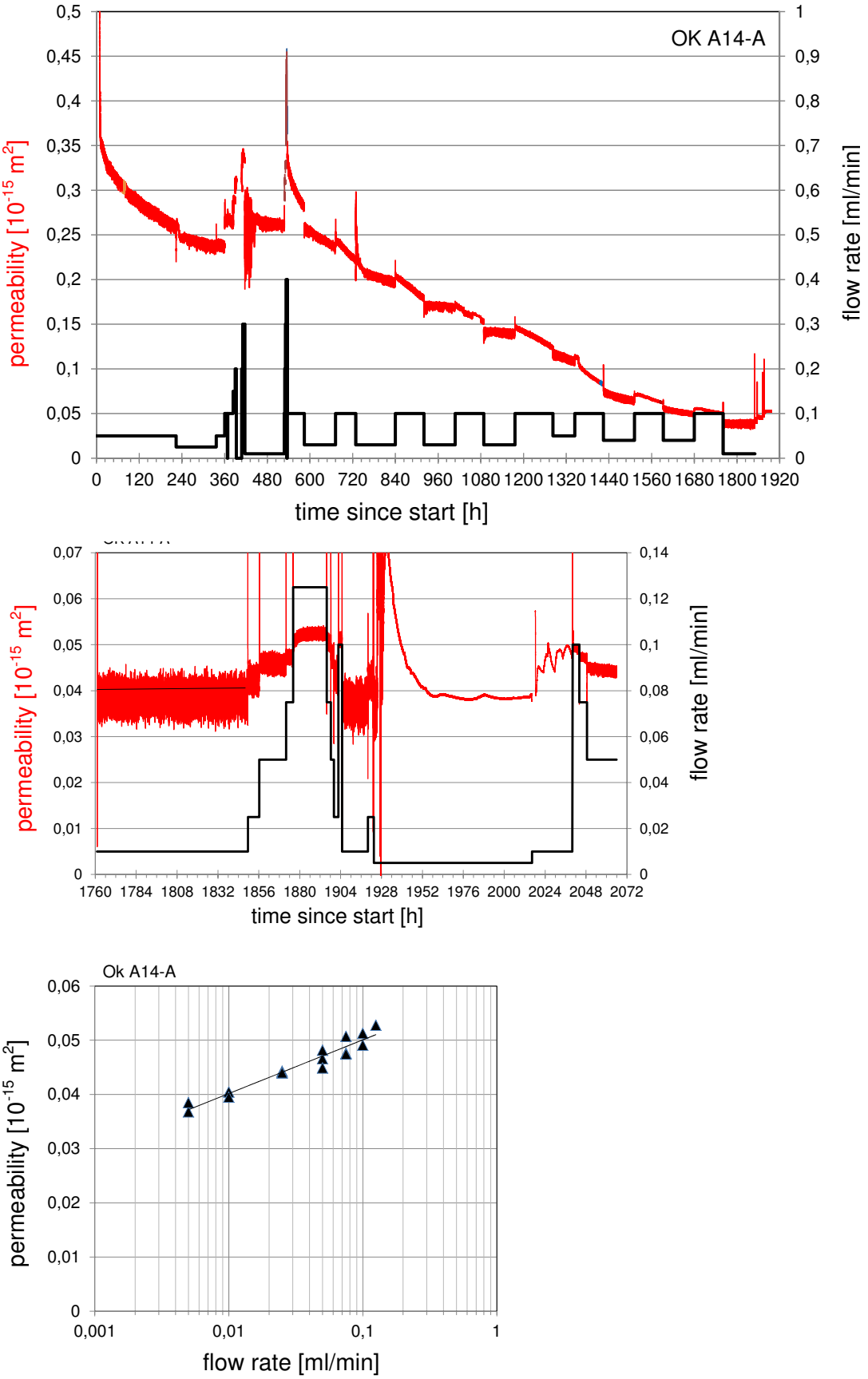

Fig. 19: Top: Permeability of Obernkirchener Sandstone (sample OK A14-A) measured with demineralized water additionally boiled for 1 hour. Center and bottom: After 1800 h permeability was constant. Then permeability was determined as a function of flow rate.

4.3 Liquid-permeability: Discussion of Results

Changes in the hydraulic properties have been studied on porous media in the field and in the lab. Reduction of permeability occurred in technical filters as well as in aquifer systems, e.g. geothermal systems in sediments or hard-rocks, sites for water or wastewater treatment, and also methods of enhanced oil recovery are effected. Decreasing permeability during flow experiments were interpreted in different ways in the literature:

1) Partial blocking of the flow path through particles: With flowing water loose particles in the pore space may be swept away. Hydraulic forces may remove weakly bonded particles. Also a flocculation is possible when temperature or chemical composition is changing. These types of particles may block or constrain the flow path at bottle necks (e.g. Kühn et al 1998) resulting in a decrease of permeability. When flow and also pressure increase, these blockages may be removed, at least in the lab. In the full space of a geological reservoir, however, particles cannot really disappear.

2) Swelling of clay minerals: Some clay minerals (Smectite, Montmorillonite) swell in presence of water. This means there is a temporarily reversible intake of water into interface layers. Molecular adhesion results from the dipole structure of the water molecule. Swelling of layers or movement of separated layers may block the flow path partially or completly. Ions of salt, such as NaCl, dissolved in water result in no or less swelling. Inside certain limitations this is reversible when fresh water is replaced by saline water (Tchistiakov 1999). Swelling is often an argument when the difference between measurements of permeability at sedimentary rocks with gas and water are discussed.

3) Growing of Biofilm inside the pore space: Biofilms are microbe aggregations of different nature. Colonies of micro-organisms may grow in thin layers on the inner surface, as flocculations in the pores or in irregular structures, such as mushrooms or walls. Microbial plugging may result from either injected or indigenous micro-organisms. These may be bacteria, fungi or algae. Water and nutrients are necessary but nutrients may already occur in the rock. Microbes may be of aerobe or anaerobe type. Even in one biofilm both types may exists together. Extracellular polymers (EPS) are often produced by bacteria. EPS is thought to strengthen the attachment of cells to a surface, forms links between cells, and provides a protective matrix which coats the bacterial cell clusters (Brydie et al. 2005).

Decreasing permeability is a typical effect of growing biofilms. Biofilms may grow also in ultra-purity water constructions, and very low quantities of nutrients may be sufficient (Flemming & Schaule 1994). Biofilms can be mechanicaly stable and resist strong shear forces through flowing water (eg. Körstgens 2003). However they can also be flexible.

4) Blockage of flow paths due to filtration of microbes from the fluid: Not only growing of new micro-organisms inside a sample may reduce permeability, but also the filtration of micro-organisms from the fluid and blockage of parts of the flow path. It is not always easy to distinguish between these different effects. Often both may be work together.

Results of the above mentioned experiment with clean quartz sandstone speak against the first two explanations. Growing biofilms may cause a continuously increasing blocking of the fluid path. A slimy film on the outside of a sample after more than two month in tap water was an additional indicator. It was expected, that rinsing the sample with hydrogen peroxide H_2O_2 should solve the problem, because H_2O_2 destroys organics. Indeed as figure 13 (inlet) shows, the gas permeability increased significantly after treatment with H_2O_2 .

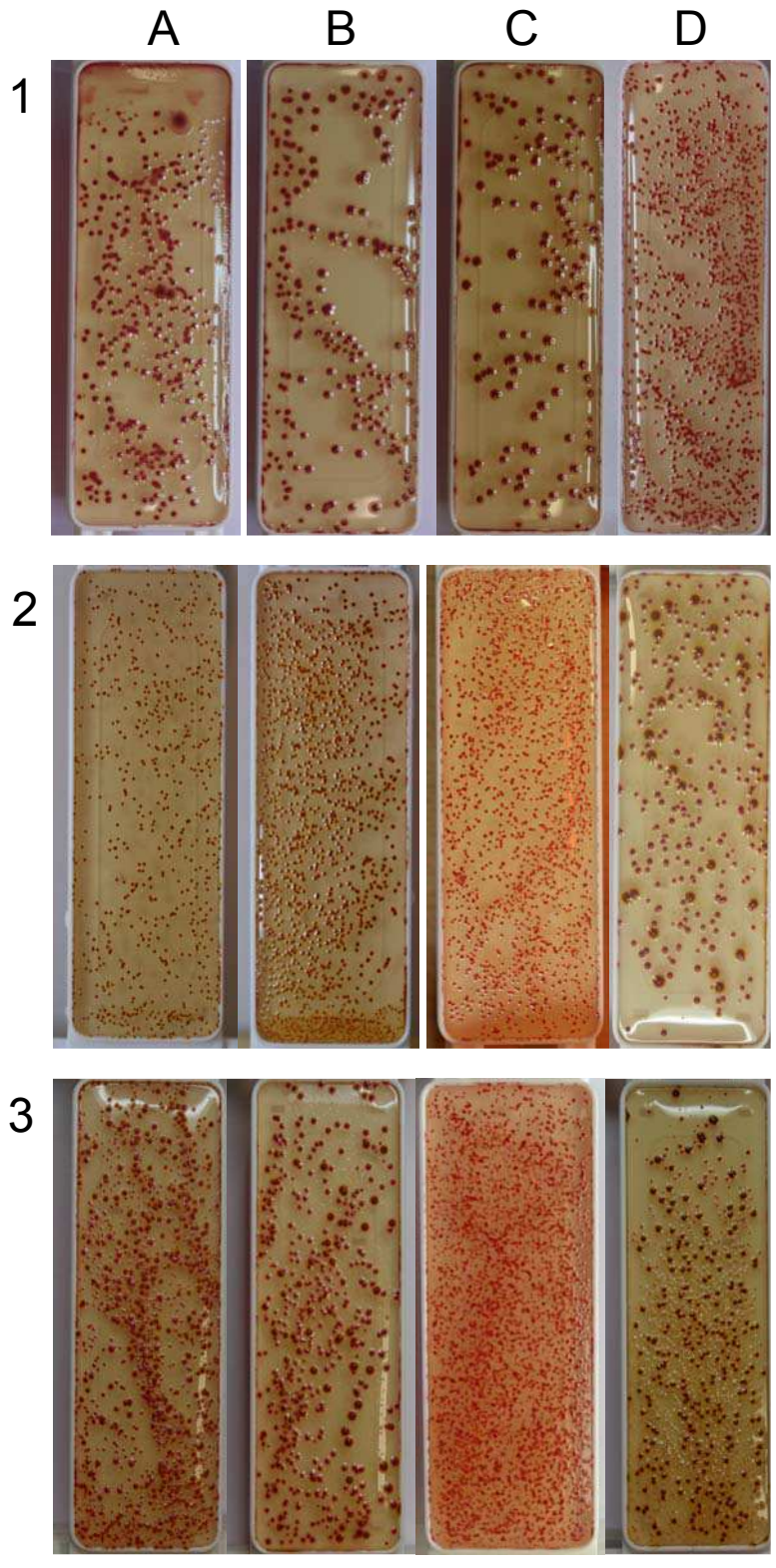

Fig. 20: Top: Samples of agar plates for detecting aerobic bacteria:
Obernkirchener Sandstone OK B1 demineralized water
A1)(left) sampling of water before auto-clave inflow
B1) outflow at 0,1 ml/min (2.4.2013)
C1) outflow at 0,2 ml/min (3.4.2013)
D1) outflow at 0,025 ml/min after 2 days at 0,002 ml/min (17.4.2013)

Center: Obernkirchener Sandstone OK A14-A demineralized and boiled water
A2) sampling water from the storage vessel
B2) outflow, short after iso-Propanol was used, 0,05 ml/min
C2) outflow
D2) outflow after weekend with 0,025 ml/min (15.7.2013)

Bottom left: Obernkirchener Sandstone OK A2 NF2 demineralized water, disinfected with ultrasonic equipment
A3) water from the storage vessel
B3) outflow 0,025 ml/min (15.8.2013)
C3) inflow behind the pump (pump purge setting 5 ml/min)(28.8.2013)
D3) outflow 0,5 ml/min (20.8.2013) also colorless dots are bacterial colonies

Bottom right: flow of demineralized water, disinfected with ultrasonic equipment - pumped with 2 µm filter at inflow – sampling at outflow of pump.

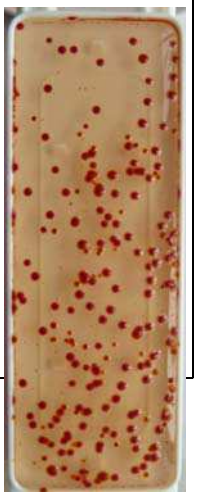

Not the single size of colonies on the agar plates, the density is indicator of concentration of aerobic bacteria in the fluid.

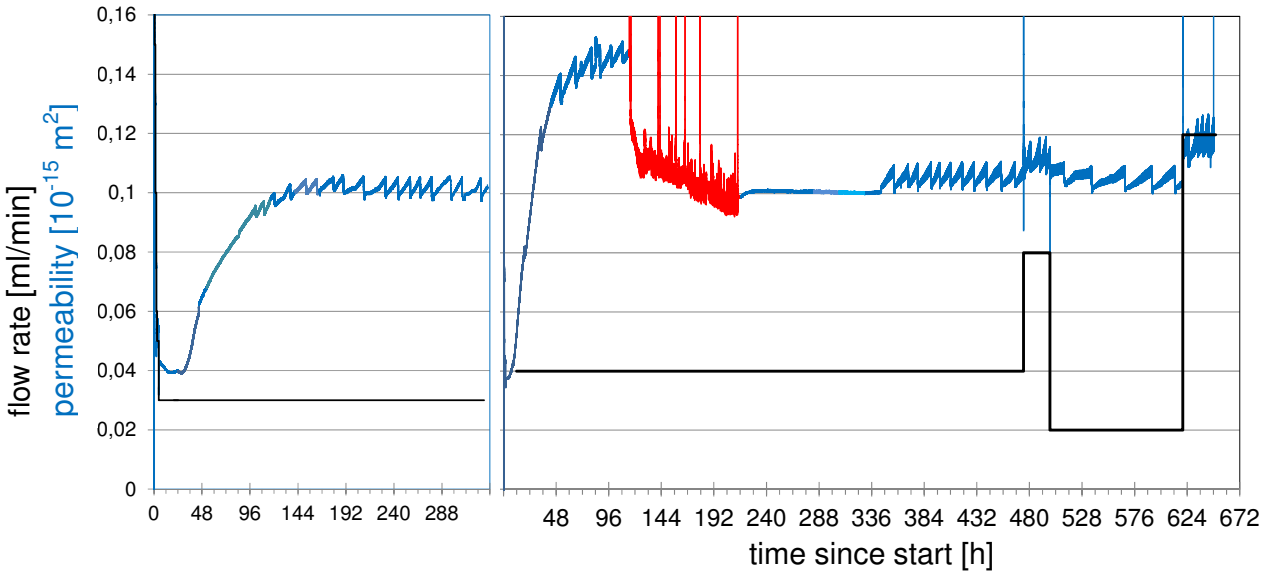

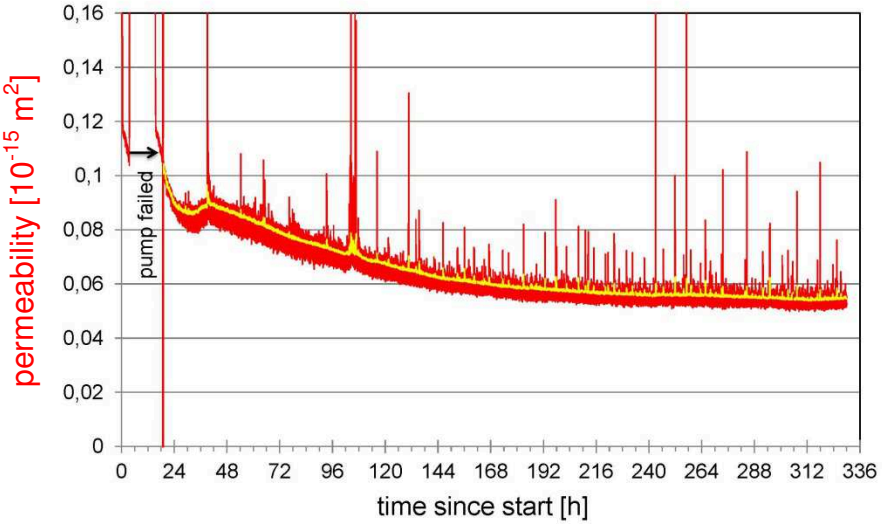

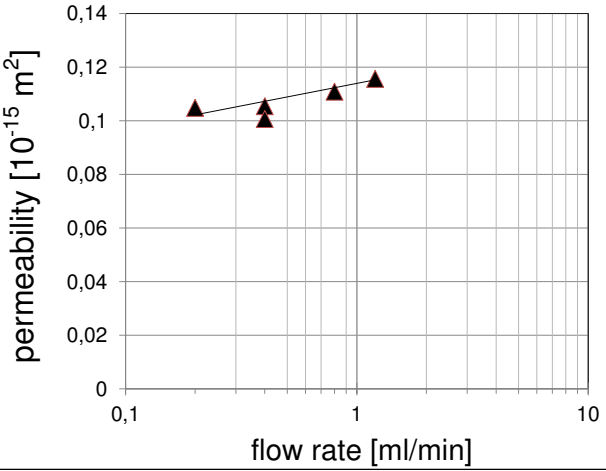

Fig. 21: Sample Obernkirchener Sandstone OK B1. Water flow through the sample with two types of HPLC pumps (blue: Knauer Smartline 1050; red: Merck-Hitachi L6200A). Top: Start with the Knauer pump, because of the sawtooth the experiment was started a second time. After getting sawtooth again (right part), we changed to the Merck pump, later on at 220 h again to the Knauer pump. After a long time without sawtooth, this effect started again. The mean permeabilites for the timespan 240 to 636 h are plotted in the permeability versus flow rate graph (bottom). Centre: The continuation of the upper graph with the HPLC pump (Merck-Hitachi), again a decreasing permeability.

Bacteria we found in all water samples. Often there is no clear difference in magnitude of bacteria in the water between in- and outflow (Fig. 20). Sometimes samples taken at the outflow and in other cases at the inflow showed a higher contamination, in other cases there were no significant differences. Some possible explanations for these observations:

1.) Bacteria from the fluid are filtrated by the sample and plug parts of the flow path, others pass through.

2.) Indigenous micro-organism are growing inside the pores, obtain energy and nutrients from the flowing water, stay inside and plug the pores; bacteria detectable by agar plates from the water more or less pass through.

3.) Bacteria produce meshes of extracellular polymers (EPS) in the pore space and these both catch and release bacteria depending on the flow rate.

The size of most single bacteria is in a range of 0.6 µm to 1 µm in diameter and between 1 µm to 5 µm in length, but smaller and larger bacteria are well known (WIKIPEDIA 2013). The number of bacteria colonies visible on the agar plate as red dots behind tested pump (Fig. 20 picture bottom right) is less than those with the usual used pump (D3). But these pump was running for more than 2 month whereas the tested pump during this sampling was running only for that water sample. This small number of colonies are in the same order as during tests in other experiments with decreasing permeability (190 instead of 280 colonies - compare with A1 on Fig. 20). But see the restrictions of the agar plates as mentioned above. So it is not definite that only smaller bacteria were possible injected into the sample by this tested pump.

Until now biofilms provide only indirect evidence. We tried to find bacteria inside the sample by cryo-SEM and optical microscopy but got no definite proof.

A decrease of permeability with decreasing water flow is unusual. Under normal conditions a flow rate might lead to a change from laminar to turbulent flow where eddies decrease the permeability. As mentioned before permeability remains constant however when using for the same sample isopropyl alcohol as fluid (Fig. 17).

In mercury intrusion porosimetry, when mercury is injected into the sample with increasing pressure, bottlenecks determine the pore characteristics. This is exactly the size we need when we look at the filtration of bacteria from the flow-through. Measured this way the main pore diameters are clearly less than 10 µm in a sample of Obernkirchener Sandstone measured by Schopper and Riepe (1986)(Fig. 22).

Judging from our data, filtration of bacteria out of the flow medium might be the main or at least an important factor for clogging of the pore space of our strongly cleaned samples. In general we think that the main reason resides in the injection of bacteria into the pore space or at least of additional bacteria or seeds into the samples is interpreted. Figure 20 suggest that in many cases inflow and outflow do not really differ significantly in the quantity of bacteria. This could be explained, if only a small portion of "large" bacteria would influence the overall behaviour or if species and anaerobic bacteria not detectable by this method cause this behaviour.

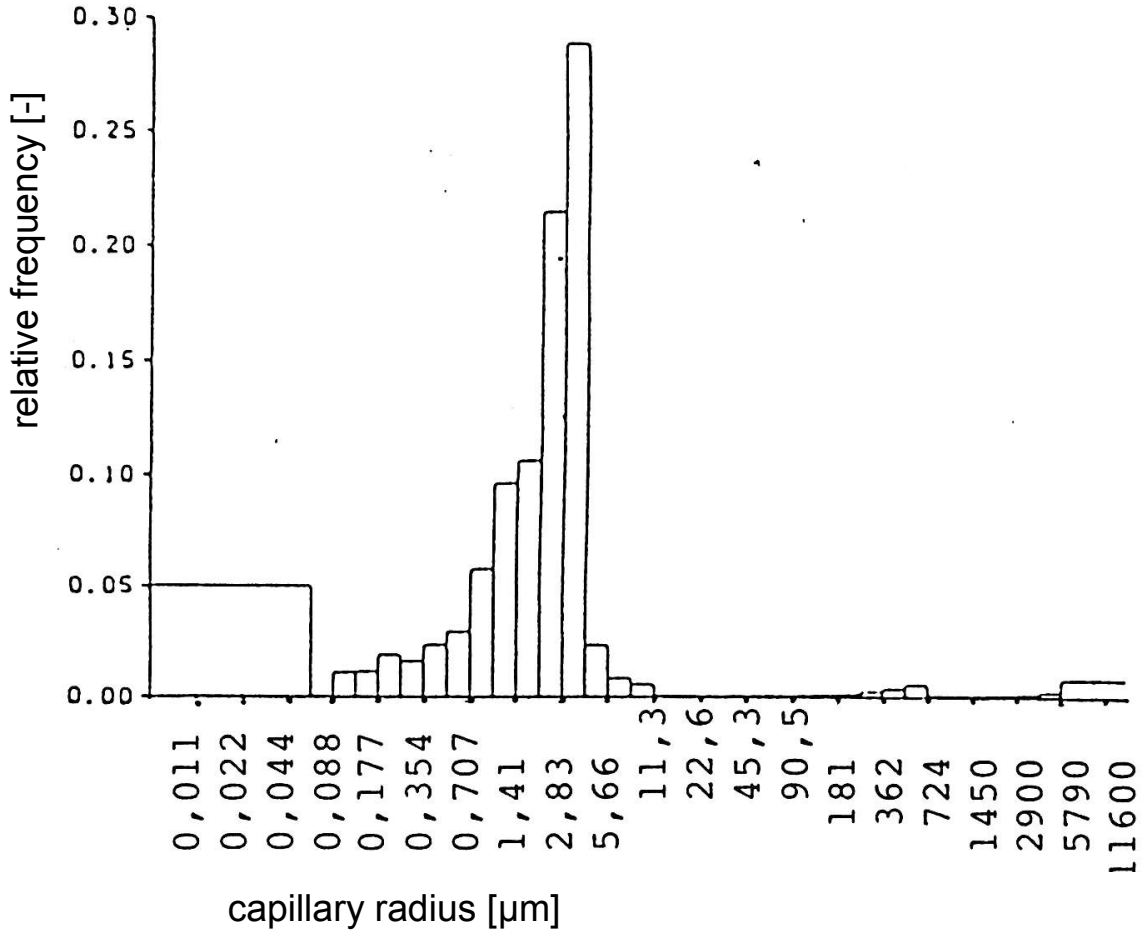

Fig. 22: Effective pore radii distribution measured by mercury intrusion porosimetry of Obernkirchener Sandstone (Ok 2/2). The sample is not from this series but can be regarded as representative (Schopper & Riepe 1986; Schütt 1992)

Laminar flow through a circular tube is described by the Hagen-Poiseuille law. From Darcy's law a simple effective hydraulic radius r can be calculated:

$$q = \frac{\pi * r^4}{8 * \eta} \frac{\Delta p}{l} \qquad q = \frac{k * A}{\eta} \frac{\Delta p}{l} \longrightarrow k = \frac{\pi * r^4}{8 * A}$$

Hagen-Poiseuille law Darcy's law

q = specific flow, rate r = pore radius, η = dynamic viscosity, Δp/l pressure gradient, l = length, A = cross section

From this equation we can estimate the overall pore radius reduction. For sample OK A2 (Fig. 13) this is on order of 45 % and OK A14-A (Fig. 19) in the order of 38 %. This estimation assumes that the pore radius distribution may be described by its mean value. But biofilms seem to grow not independently of pore sizes, Torbate et al. (1985) states that microorganisms preferentially plugged larger pore entrances in Berea sandstone and these are more important for flow through than the smaller ones.

5. Conclusion

We built an experimental set-up which allows the measuring of physical rock properties at elevated pressures and temperatures: Fluid rock permeability and elastic p- and s-wave velocities. Knowledge of these properties at reservoire conditions is required successfully modeling hydrocarbon, geothermal, and mineral reservoirs, as well as subsurface storage of nuclear waste or CO_2.

Measurements of permeability using Argon gas (measuring range $5x10^{-18}$ m^2 to 10^{-12} m^2) yielded in the expected results. That also holds for the p- and s-wave velocity experiments. But measurements of permeability based on water resulted in unexpected dependencies:

1. a long-term decrease of permeability: at end of experiments, permeability is only about 10 % of its starting values (Fig. 13 & 19).

2. At the end of the experiments, low permeabilities were found to increase with flow-rate.

The most likely reason for these findings are micro-organisms in the pore space. Micro-organisms could not be definitely verified as reason for clogging of pore space or the decrease of permeability. Microbial cells exist even in the cleanest water if the environmental condition tolerate life. Under favourable conditions micro-organism will grow and form a biofilm. On this aggregation organisms may attach or detach. Thus, is not surprising that bacteria are found both in the in- and out-flowing water of the studied samples, as shown by the agar plates.

We found no bacteria directly inside the samples, maybe because of insufficient experience in this field. The following details point to this explanation: At first the different behaviour of water and propyl alcohol, this speaks against a displacement of micro particles and flow blockage at bottle necks. The behaviour after cleaning with hydrogen peroxide indicates that swelling of clay minerals is no important reason for rock of such low clay content.

Experiments with bacteria are often performed with selected bacteria fed with nutrients (e.g. Cunningham et al. 1991). This resulted in drastic permeability decrease within hours or few days. We did not use nutrients for increasing the bacteria growth.

Compared to the pore space of some 5 cm^3 to 6 cm^3 in our Obernkirchener Sandstone samples we pumped always large values of water through the samples. In first experiment (Fig. 13) more than 5000 cm^3, in the last one (Fig. 19) more than 3000 cm^3. The velocity of water through these samples lie typically between 0.1 mm/min (0.01 ml/min) and 1 mm/min (0.1 ml/min). The long duration of each experiment rinse many bacteria through a sample even when these are in low concentration in water. Or when only few are filtrated out of the flow-through, may be 10 % or 20 % , we saw no difference between in and outflow identified in the agar plates.

Some further experiments may support or dispose this explanation in the future:

1.) If autoclaved water is flushed through a strongly cleaned sample no change of permeability should occur.

2.) In flow-through of water with nutrients, a faster change should occur than in the previous experiments.

3.) An injection of bacteria together with nutrients should result in a very fast biofilm generation.

6. References

Branda, S.S., Ä. Vik, L. Friedman & R. Kolter (2005): Biofilms: the matrix revisited. TRENDS in Microbiology 13: 20-26.

Brydie, J.R., et al. (2005): The µ2M project on quantifying the effects of biofilm growth on hydraulic properties of natural porous media and on sorption equilibra: an overview. Geol. Soc., London, Spec. Pub. 2005, Vol 249: 131-144.

Cunningham, A.B., W.G. Characklis, F. Abedeen & D. Crawford (1991): Influence of Biofilm Accumulation on Porous Media Hydrodynamics. Evironm. Sci. Technol. 25: 1305-1311.

Darcy, H. (1856): Les fontaines publiques de la ville de Dijon, Dalmant, Paris.

Flemming, H.C. & G. Schaule (1994): Mikrobielle Werkstoffzerstörung – Biofilm und Biofouling: Biofouling. Werkstoffe und Korrosion 45: 29-39.

Kilmer, N.H., N.R. Morrow & J.K. Pitman (1987): Pressure sensitivity of low permeable Sandstones. J. Petrol. Sci. Engineering 1: 65-81.

Körstgens, V. (2003): Die mechanische Stabilität bakterieller Biiofilme: Eine Untersuchung verschiedener Einflüsse auf Biofilme von Pseudomonas aeruginosa. Diss., Universität Duisburg-Essen.

Kühn, M. J.-F. Vernoux, T. Kellner, M. Isenbeck-Schröter & H.D. Schulz (1998): Onsite experimental simulation of brine injection into a clastic reservoir as applied to geothermal exploitation in Germany. Appl. Geochemistry 13: 477-490.

Schön, J.H. (1996): Physical properties of rocks. Pergamon, Oxford.

Schopper, J.R. (1982): 2.3 Permeability of rocks - Permeabilität der Gesteine. In Hellwege (Ed.): Landolt-Börnstein/Zahlenwerte und Funktionen aus Naturwissenschaft und Technik, Group V, Geophysic and Space Research, Vol. 1 Physical Properties of Rocks, Subvol. A: 184-303.

Schopper. J.H. & L. Riepe (1986): Experimental and theoretical petrophysical investigations on relations between the inelastic absorption in porous rocks and other petrophysical and reservoir parameters. p. 239-276. In Burkhardt, H., J. Paffenholz & R. Schütt (Ed.): Absorption of seismic waves in hydrocarbon exploration. Deutsche wissenschaftliche Gesellschaft für Erdöl, Erdgas und Kohle e.V. (DGMK), Hamburg.

Schütt, R. (1992): Experimentelle und theoretische Untersuchungen zur Dämpfung und Geschwindigkeit von Kompressions- und Scherwellen in Sedimentgesteinen bei Ultraschallfrequenzen. Doctoral Dissertation, Technische Universität Berlin, Berlin.

Schwartz, H.E. & R.G. Brownlee (1985): Comparison of Dynamic and Static Mixing Devices for Gradient Micro-HPLC. J. Chromatographic Sci. 23: 402-406.

Tanikawa, W. & T. Shimamoto (2009): Comparison of Klinkenberg-corrected gas permeability and water permeability in sedimentary rocks. Int. J. Rock Mech. Mining Sci. 46: 229-238.

Tchistiakov, A.A. (1999): Effect of flow rate and salinity on sandstone permeability. Bulletin d'hydrogéologie 17 - Special issue: European Geothermal Conference Basel '99, Proceedings Vol. 2: 189-197.

Torbai, H.M., R.A. Raiders, E.C. Donaldson, M.J. McInerney, G.E. Jenneman & R.M. Knapp (1986): Effect of microbial growth on pore entrance size distribution in sandstone cores. J. Industrial Microbiology 1: 227-234.

WIKIPEDIA 2013, German Version, "Bakterien", http://de.wikipedia.org/wiki/Bakterien, Wikimedia Foundation, San Francisco, CA, retrieved 29.8.2013

Notes:



E.ON Energy Research Center Series

ISSN: 1868-7415
First Edition: Aachen, January 2014
E.ON Energy Research Center,
RWTH Aachen University

Mathieustraße 10
52074 Aachen
Germany

T +49 (0)241 80 49667
F +49 (0)241 80 49669
post_erc@eonerc.rwth-aachen.de
www.eonerc.rwth-aachen.de